(Received 24 October 2023, Accepted 20 December 2023, Scheduled 22 January 2024)

Millimeter Wave Antennas: A State-of-the-Art Survey of Recent Developments, Principles, and Applications

Reena Aggarwal[1], Ajay Roy[1], and Rajeev Kumar[2, *]

[1] School of Electronics and Electrical Engineering, Lovely Professional University, Punjab, India
[2] Chitkara University Institute of Engineering and Technology, Chitkara University, Punjab, India

ABSTRACT: The increasing volumes of data generated by social networking, cloud computing, e-commerce, and online video broadcasting necessitate the implementation of higher data rates. As the current 4G network encounters congestion and potentially struggles to accommodate the substantial data demand, there is a growing interest in millimeter wave (mmWave) technology. The 30–300 GHz mmWave spectrum is characterized by its broad bandwidth and low latency; it is having many applications in communication domains, also includes 5G cellular. Despite its atmospheric attenuation and non-line-of-sight (NLOS) propagation, the majority of nations have begun to implement mmWave 5G in the band of 28/38 GHz as a result of its reduced path loss exponent, minimal signal spread, and decreased atmospheric attenuation. While the patch antenna (single-element) is a compact and easily transportable choice for mmWave applications, its radiation efficiency, gain, and bandwidth are all subpar. Array antennas have effectively addressed these limitations by exhibiting significant enhancements in bandwidth, gain, and radiation efficiency. It is still limited in the maximum data rates it can accommodate. The rate of data can be increased by a factor of one thousand using Multiple-Input-Multiple-Output (MIMO) technology, which is enabled by geographical diversity and multiplexing techniques. As a result, the comprehension of structures of MIMO antennas operating at mmWave is imperative for the continued enhancement of performance. In comparing the efficacy of these designs, bandwidth, isolation, efficiency, gain, and radiation pattern are considered. In this paper, the most recent planar MIMO antenna designs, which are categorized as defected ground structures, Slot/Patch/Stub, MIMO Antenna Array, Dielectric Resonator Antenna, and Meta-Surface/Metamaterial Structures, are described. This paper also addresses the effects that slots, partial ground, and decoupling structures have on levels of isolation, bandwidth, and impedance matching. A comprehensive analysis of the design considerations and subsequent advancements is also provided in this paper.

1. INTRODUCTION

Due to the constant demand for data, network providers must work harder to provide high-speed mobile internet. Most apps are hosted in the cloud or online, which demands continuous data speeds and low latency [1]. 5G technology makes this possible. Many nations are building 5G infrastructure to better serve their customers. The Telecommunications Regulatory Authority of India (TRAI) just released 26 GHz mmWave spectrum for 5G in India, so vendor services may start soon [2, 3].

The ITU-International Telecommunication Union predicts almost five billion internet users by 2023 [4]. This group comprises 67% of the global population. The world will have 5.4 billion internet users by December 31, 2023 [5]. Figs. 1 and 2 show global internet usage and average consumption of data over the past two decades. Due to its limited bandwidth and growing user base, 4G LTE-Long Term Evolution data support capability has reached to its saturation point. Despite its limits, mmWave for 5G could improve data throughput due to its large bandwidth [6]. Most nations are deploying 5G in Group 30 and 40 channels at mmWave, per WRC recommendations [7]. Forge et al. in [8] presented the 5G deployment plans and policies for the low income countries based on research on 5G-enabled states. This research focused on 5G-implemented nations.

Wireless communication technology is expanded by the mmWave's large bandwidth at 30–300 GHz [9]. The mmWave wavelength is 1–10 mm, which is Extremely High Frequency (EHF) according to ITU regulations. The FCC has improved the least mmWave bandwidth to 400 MHz [10] because to the longer wavelength and wider spectrum, compared to 4G (LTE). Fig. 3 shows mmWave benefits.

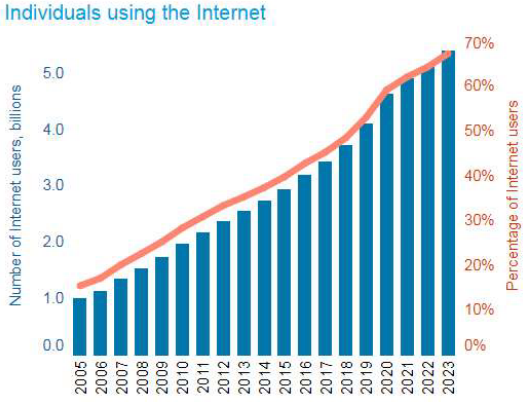

FIGURE 1. Internet usage statistics given by ITU [4].

* Corresponding author: Rajeev Kumar (rajeev.kumar@chitkara.edu.in).

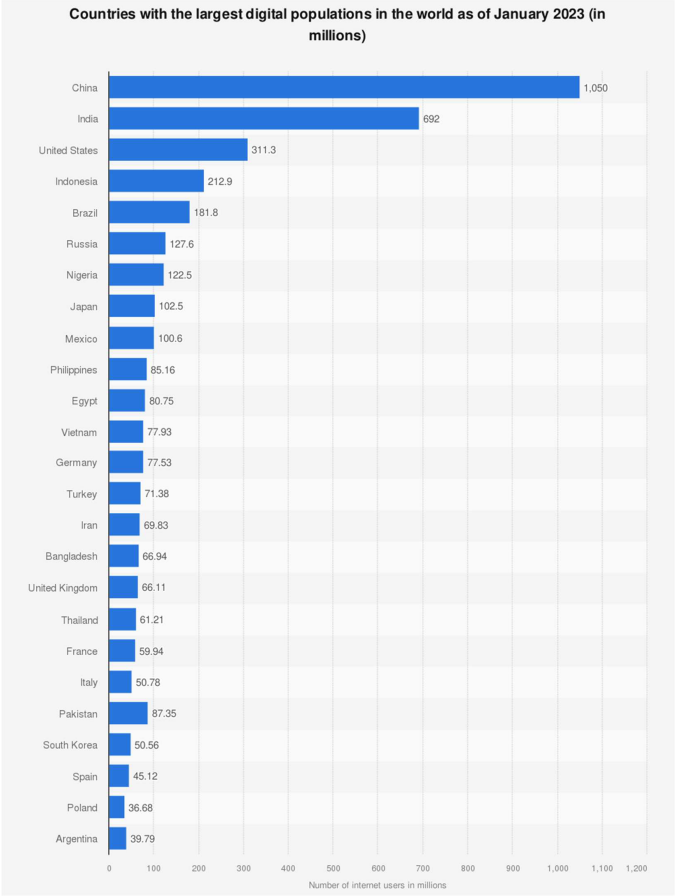

FIGURE 2. Internet usage statistics of different countries [11].

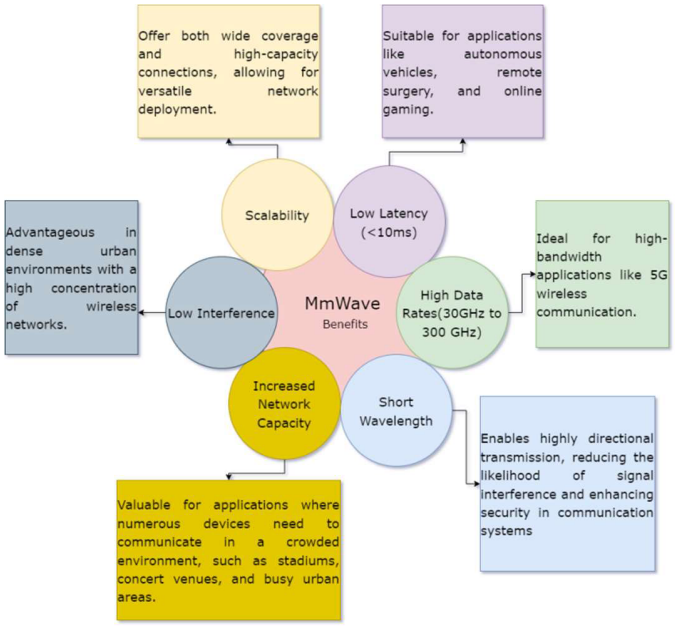

FIGURE 3. Advantages of milli-meter wave.

The signal baud rate may transport more information due to mmWave's high carrier frequency, resulting in a higher rate of data (bits/sec/Hz) & reduced the time of buffering while producing high-quality films [12]. Cellular communication exploits frequency reuse through cell splitting and sectoring to expand network coverage due to the mmWave's limited range [13]. As shown in Fig. 4, other mmWave applications include 5G and small cell concept, HD video, Satellite Communication, Automotive, Body Scanner, Radar and image sensing, headsets of virtual reality, medical-mmW therapy, military, IEEE 802.11ad WiGig technology and IoT [14].

Besides its benefits, mmWave has numerous limitations, including air attenuation from gaseous losses (such as water vapor and oxygen absorption of radio signals) rain, and propagation path losses [15]. Above 10 GHz, atmospheric H_2O and O_2 molecules impede mmWave signals. The signal is greatly attenuated by H_2O at the frequencies of 20 GHz, 200 GHz, and 250 GHz and O_2 at 4 GHz and 100 GHz. Due of its shorter wavelength than rainfall or plants, mmWave signals scatter. Another drawback of mmWave is that its shorter wavelength prohibits it from traveling through dense structures, limiting it to LOS communication [16]. NLOS mmWave channel measurement studies in (urban/suburban) areas have given low route loss exponent and signal spread, making it popular for 5G applications. High gain and directivity are dependent on the antenna in wireless communication systems [17–19]. An early mmWave study [20] suggested a reflector design, lenses, arrays, and horn technique to boost antenna gain.

Moreover, the significant influence of millimeter-wave antennas on system design becomes evident through detailed examination of their technological complexities. As scholars confront the obstacles presented by elevated frequencies, namely those over 30 GHz, they explore inventive approaches such as sophisticated beamforming methods and phased array systems to surmount constraints in signal transmission. The enhancement of millimeter-wave communication efficiency necessitates a rigorous focus on optimizing antenna design factors, such as substrate materials, radiation patterns, and gain. Concurrently, the pursuit of reducing size and achieving seamless integration with developing technologies demonstrates a dedication to modifying millimeter-wave antennas to suit the changing environment of communication standards. In [15–20], scholars strive to not only tackle distinctive obstacles associated with higher frequencies but also use the whole capabilities of millimeter-wave communication systems in the context of our swiftly progressing technological epoch.

This work presents a thorough investigation of mm-Wave MIMO antennas, encompassing a range of technical considerations aimed at improving their overall performance. The conversation commences with a comprehensive analysis of mmWave MIMO antennas, encompassing methodologies aimed at enhancing isolation and mitigating surface wave

FIGURE 4. Milli-meter wave's applications.

current. The focus of this study is to highlight the advantages of Dielectric Resonator Antennas (DRAs), while also providing a comprehensive analysis of efficient feeding methods and strategies for reducing their size. This study examines advanced design techniques that might enhance individual direct radio access (DRA) gains. It provides useful insights for Radio Frequency (RF) front-end designers that aim to choose antenna topologies that fit with specific performance metrics, including frequency response, gain, and polarization. Main contribution of the article:

- It gives an overview of mmWave MIMO antennas as well as different ways for improving isolation and lowering surface wave current.
- The benefits of DRAs are detailed in the manuscript, along with the most effective antenna feeding and size reduction approaches. Additionally, advanced design methods to improve individual DRA gains are examined. Radio frequency (RF) front-end designers receive help on selecting antenna topologies to meet desired performance in frequency response, gain, and polarization.
- Different approaches of MIMO array are discussed to focus considerable improvement in data speeds and network efficiency that results from their capacity to transmit/receive many data streams simultaneously.
- Examining the structure of the metamaterials help to improve design performance.
- In addition to their impact on the performance of the antenna, it examines the significance of slots/ slits, stubs, patch and DGS in designing of the antenna structures.
- It examines the advantages of current designs and the difficulties in enhancing the antenna structure for improved MIMO antenna performance.

The exploration of developing antenna structures encompasses not only materials and structures, but also the examination of individual parts such as slots, slits, stubs, patches, and defective grounds, which hold significant importance. This study goes beyond the assessment of the benefits offered by existing designs, and instead focuses on the inherent problems associated with upgrading antenna structures in order to achieve greater performance in MIMO antennas. This detailed study serves as a significant resource for researchers and RF front-end designers, offering a nuanced grasp of the various tactics and factors involved in improving millimeter-wave MIMO antenna systems.

2. MILLI-METER WAVE ANTENNAS

Antennas like planar [21], transparent [22], planar with metamaterial loaded [23], tapered slot [24], bow-tie [25], and other single-element mmWave antennas are the simplest and most compact. Single-element structures have low gain, bandwidth, and efficiency. The 5G mobile app requires tiny beam-directed radiation, yet the radiation pattern is generally omnidirectional. Therefore, array antennas are able to solve these problems [26] because they offer a multiple benefits, including wide-angle beam scanning, adaptive beam-forming, broad bandwidth, and enhanced gain etc. [27]. When designing a planar array, leave x and y radiating components spaced apart. This reduces side and grating lobes [28]. Line spacing should be $\lambda/2$ or less (typically). Broad-beam scanning uses rows, columns, or subarrays of radiating arrays. Phase shifters route subarrays individually. Array designs have better bandwidth, good gain, and radiation than designs of single-element but no data rate advantage. Millimeter-wave MIMO antennas can do this [29, 30]. Thus, this review discusses millimeter Wave MIMO antennas. Since planar MIMO antennas provide higher gain, bandwidth, directivity, and data transfer rates, The 5G devices that employ these designs which are easy to incorporate due to its low profile nature. Fig. 5 shows the classification of MIMO antennas through design structure. Section 1 gives the introduction of the paper, Section 2 provides the insight about the Milli-Meter Wave Antennas and the Section 3 examines MIMO antenna for mmWave applications (slot/patch/stub antennas, defected ground antennas, MIMO Antenna Array, dielectric resonator antennas (DRA), and Meta-surface/metamaterial-based designs). The remaining manuscript is ordered as follows. The Technical Challenges, Scientific & Technological Trends: in Millimeter Wave Antennas are described in Section 4 and Section 5 provides the conclusion the paper.

MIMO antennas aid in heavily crowded areas where LOS is impossible. Multipath fading occurs when the signal passes across multiple paths in-phase or out-of-phase [31]. MIMO antennas with combiners boost signal-to-noise ratio (SNR) and diversity gain, reducing multipath (Fig. 6). Selection, switched, equal-gain combining (EGC), and maximal-ratio combining (MRC) are diversity combiners. Selection combining chooses the highest SNR branch at any time. Switched combiners choose the branch signal with the lowest threshold. EGC cophases branch signals. MRC gives each branch phase weights to make the output equal the SNRs [32].

In the beginning, MIMO antennas increase spatial variety to combat channel fading. In a Rayleigh fading scenario, m antennas provide data to n independent receiving antennas via separate paths [33]. Spatial Diversity (nm) is the maximum diversity gain in this situation. Spatial multiplexing can increase data rate [34, 35]. This happens when many antennas offer independent data. The non-asymptotic technique [36] calculates the numerous of transmitting antennas needed to enhance the channel capacity. Also author in [37] gives the non-asymptotic analysis of massive MIMO under different wireless scenarios.

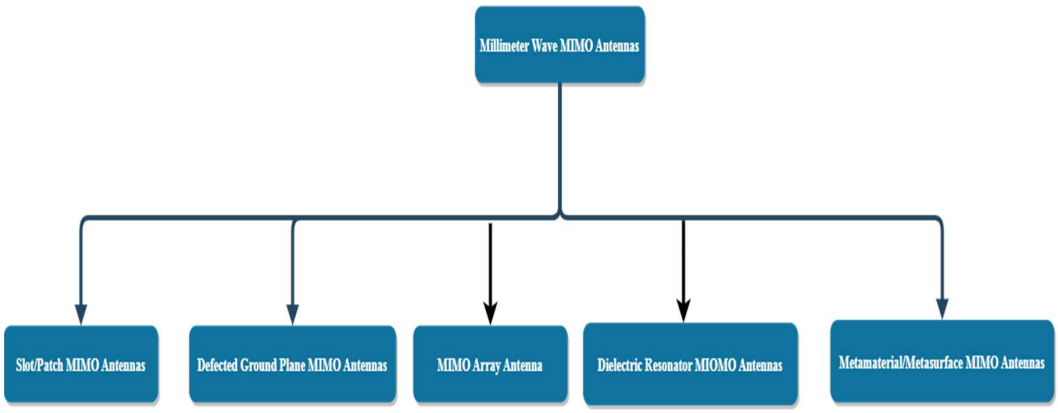

FIGURE 5. Types of MIMO antenna for Millimeter Wave (MMW).

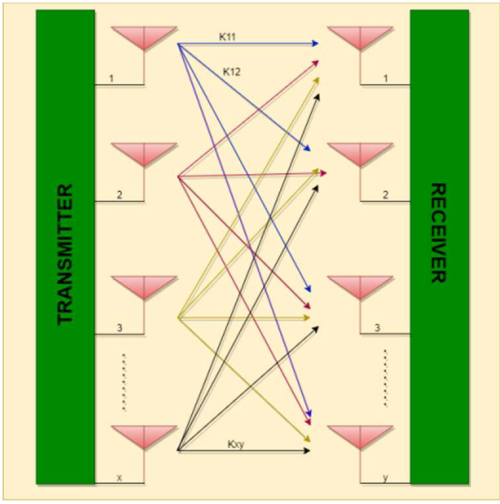

FIGURE 6. Overview MIMO antenna.

The coupling loss and coefficient of correlation among MIMO designs must be minimized. At four antennas at the working frequency, mutual coupling loss becomes significant [38]. This occurs when antenna spacing is smaller than 0.2λ. Diversity parameter measurements prove MIMO antenna performance. These include Envelope Correlation Coefficient (ECC < 0.5), Mean Effective Gain (MEG -3 to -12 dB), (DG — Diversity Gain is 10 dB), (CCL — Channel Capacity Loss is 0.4 b/s/Hz), (TARC — Total Active Reflection Coefficient is -10 dB), and Multiplexing Efficiency (0 ECC is Envelope Correlation Coefficient. The References [39–41] provide the equations and lowest allowable value for each parameter.

Figure 7 shows that the Release-19 of the 3GPP standards focuses on advancing 5G MIMO antennas, integral to 5G network evolution. The standards encompass configurations like Massive MIMO, utilizing numerous antennas for enhanced spectral efficiency. Emphasizing beamforming techniques, the standards ensure optimized signal direction for improved coverage and reliability. Addressing both Sub-6 GHz and millimeter-wave bands, specifications guide the deployment of 5G MIMO antennas across diverse frequencies. Advanced technologies like beam-steering and beam-switching are detailed for adaptable communication in varied conditions. Spatial multiplexing methods enable simultaneous transmission of multiple data streams, crucial for achieving higher data rates. The standards prioritize interoperability, facilitating seamless integration of antennas from different vendors within the 3GPP framework. Moreover, they consider the integration of 5G MIMO antennas with emerging technologies like IoT, contributing to a comprehensive and interconnected communication ecosystem. For precise details, reference to the official 3GPP documentation is recommended [42].

3. MIMO DESIGNS FOR MILLI-METER WAVE APPLICATIONS

Different types of designs have been specifically developed for mmWave (millimeter wave) applications that utilize (MIMO) technology. This manuscript classifies MIMO designs according to their structural design, including slot/patch/stub antennas, defected ground antennas, MIMO Antenna Array, dielectric resonator antennas (DRA), and Meta-surface/metamaterial-based antennas as given in Fig. 5. In this study, the analysis of MIMO antennas is conducted with a focus on many parameters including bandwidth, gain, efficiency, and pattern of radiation (half-power-beamwidth).

3.1. Slot/Patch MIMO Antennas

Many of the planar patch designs use one substrate, making them cheaper and simpler. For multi-band resonant frequency and bandwidth, the planar design uses the slots [43, 44]. Also, Rectangular slots [45], E-shape [46–48], U-shape [49, 50], fractal-shape [51, 52], annular slots [53], Dual-mode slot-patch [54], U-shaped patch-slotted (four-element) design [59], and many more [53–61] dominate the radiating plane of the design. To maximize radiation efficiency, match the port at input, of the radiating element, with the microstrip feed line of 50 Ω, which depends on its width. This section compares slot MIMO antennas.

A SIW-substrate-integrated waveguide, triple-port mmWave annular slot antenna is designed [53]. Due to its easy integration and strong port isolation, the antenna under study seems

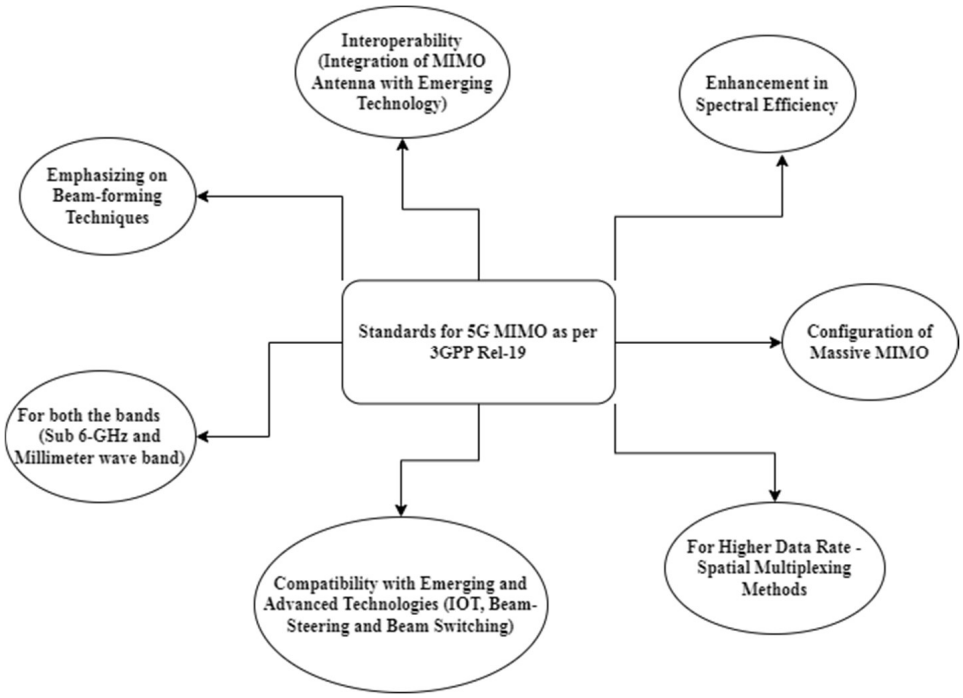

FIGURE 7. 3GPP standards for 5G MIMO antennas release-19 [42].

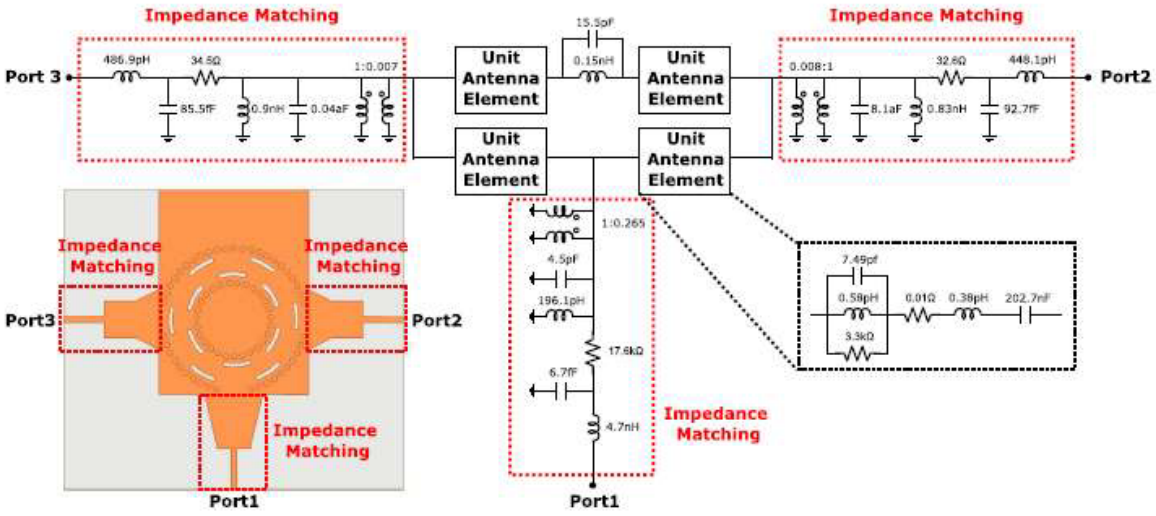

FIGURE 8. Equivalent model [53].

promising as a monostatic simultaneous transmit and receive (STAR) antenna.

Circular design and substrate integrated waveguide (SIW) transmission line technologies reduce the device's footprint. This antenna works on 5G (mmWave in-band full-duplex-IBFD systems) due to port isolation. Monostatic STAR antennas are compatible. Since IBFD allows simultaneous transmission and reception (STAR) on the same frequency, it could increase wireless communications spectral density and system capacity. To isolate TX and RX signal channels by 90 to 120 dB is the biggest problem for IBFD systems. Such separation requires more than antenna design. Further self-interference cancellation methods are advised. Increasing antenna isolation can minimize RF and digital successive interference cancellation (SIC) requirements. This architecture in [53] permits any combination of the 3-ports for the Tx and Rx without physical changes. The antenna could be a transmitter-only or receiver-only component in a phased array-5G MIMO system. The single port excitation case has 4.71 dBi maximum gain, whereas the two port case has 8 dBi. Both have 88.78% radiation efficiency. From frequency range 27.5 GHz to 28.05 GHz, the lowest -10 dB bandwidth is 0.55 GHz. The ECC for this bandwidth is below 0.002. The authors also say that the 3D simulated and comparable model results in Fig. 8 agree well.

A novel two-mode slot-patch design for Ka-band frequencies is suggested [54]. This study increases the bandwidth of a design driven by an open-ended substrate integrated coaxial line by combining the resonant modes of a slot and four patches. This architecture delivers stable, unidirectional radiation. The 1×8 array antenna has the uneven power feeding network. The system has a resonance frequency of 27 GHz and a $0.52 \times 0.52\lambda_0$ size. Individual elements have 7.9 dBi max gain, whereas the array (1×8) has 15.4 dBi. Side lobe is under -18 dBi, bandwidth 23%. A unique design with 2 linked resonances and wideband continuous unidirectional emission is created by placing virtual shorting pins, at the inside corners of the patches in [54].

A high-isolation integrated MIMO system for sub-6 GHz and mmWave frequencies is reported in [55]. The design includes four triple-band monopoles and four dual-band dual-function millimeter wave. Monopole antennas decoupled with 24 and 28 GHz (5G) millimeter wave antennas increase sub-6 GHz isolation. The design isolates the lower band by -22 dB and exhibits 0.284 envelope correlation. The design operates at 4G LTE, 5G and WLAN with the bandwidth of 1.75 GHz and 1.08 GHz respectively. Peak gain of the design are 3.47, 2.65, and 5.64 dBi at 2.5, 3.5, and 5.2 GHz frequency of the design. Millimeter-wave antennas with 8.5 and 11.4 dBi gain at 24 and 28 GHz and 7 GHz bandwidth. The simple and compact design, good gain, and wide bandwidth make it appropriate for WLAN, 5G, and 4G LTE. Sub-6 GHz decoupling is added to mmWave radiation in this patch antenna. External decoupling is no longer needed to detach monopole antennas. Isolation is achieved through the orthogonality of ground plane slots and antenna elements.

An asymmetric flare-shaped patch MIMO antenna with two inputs and two outputs is proposed for millimeter-wave communication systems in [56]. MIMO design achieves -10 dB return loss across 20–40 GHz with greater than 20 dB isolation between the design components. Return loss, gain, effective coupling coefficient, and radiation pattern for the proposed MIMO design are realized by the authors. The design meets MIMO diversity performance with two antenna elements by isolating signals by more than 20 dB and amplifying them by 8.17 dB with an ECC value of < 0.0001. Single-element antennas have a maximum gain of 8.14 dB and an impedance bandwidth of 10 dB at 20–40 GHz. To obtain higher than -20 dB isolation across the frequency spectrum, the best-optimized value is 11.2 mm between the two elements [56].

An innovative compact tree-shaped planar quad element MIMO antenna is shown in [57]. A four-arc radiating element provides a wide bandwidth response. The MIMO system of quad element, -10 dB criteria impedance bandwidth (from 23 GHz to 40 GHz), with port isolation exceeding 20 dB. The patterns of radiation at 28 GHz, 33 GHz, and 38 GHz yielded max. gains of 10.58 dB, 8.87 dB, and 11.45 dB. The antenna design's improved gain may reduce higher-frequency air attenuations. At millimeter wave frequencies, the MIMO antenna has an efficiency of about 70%. In addition, MIMO systems meet the conditions of MEG being less than 3 dB and ECC less than 0.5. The architecture aids fast data transmission. The suggested arrangement also arranges MIMO antenna elements orthogonally. To prevent mutual interference between MIMO antenna parts, diagonal components are built anti-parallel. The antenna elements' ground surfaces are also coupled to maintain consistent voltage in the proposed MIMO antenna system.

The authors use an interconnected 3 and 4 element wideband MIMO design for millimeter-wave 5G applications in [58]. This was done by numerical simulations and experiments. To generate MIMO antennas with three or four elements, the unit element is carefully created and positioned utilizing orthogonal rotation. An interconnected ground for both cases improves the resonator's practicality. At the lowest operational frequency, the MIMO antenna dimensions are $(0.95\lambda \times 3\lambda)$ for case 1 and $(2.01\lambda \times 1.95\lambda)$ for case 2. Both designs have 43% impedance bandwidth from 26 to 40 GHz. The three- and four-element MIMO antennas also work well in millimeter-wave 5G applications.

Single-element design optimization for wideband frequency resonance was the authors' initial emphasis in [58]. This single-element configuration allowed the development of 3 and 4 element MIMO designs. Both the designs have a connected the plane of ground that meets real-world use requirements. Using a connected ground plane design provides over 20 dB of isolation. As described in [58], this design has advantageous diversity metrics, including an ECC below 0.02 and the value of DG above 9.9.

A compact-slotted four-element planar monopole MIMO design for 5G mmWave N257/N258 and N262 bands is presented [59]. The design has 4 U-shaped patches on top of the dielectric layer and a slotted ground underneath. To enhance the MIMO antenna impedance, add a $1.3\,\text{mm} \times 0.2\,\text{mm}$, rectangular strip and two slots to each radiating element. The U-shaped slotted radiating components provide the initial operational band at a frequency of 27.1 GHz (25.9–27.8 GHz). Carving hexagonal grooves on the ground creates the 2nd operating band at a frequency of 48.7 GHz (47.1–49.9 GHz). By placing radiating elements and slots orthogonally on the ground, the antenna isolates > -27 dB. At 27 GHz and 48.7 GHz, the bands of N257/N258 and N262 achieved respectively. The design exhibits stable radiation patterns, > 5.95 dBi peak gain, $> 90\%$ radiation efficiency, $< 10^{-6}$ envelope correlation coefficient, ≤ -10 dB total active reflection coefficient, < 0.03 bits/s/Hz channel capacity losses, and ≤ -3.

The L-shaped microstrip line antenna in [60] has stubs (fishtail) on one side. Adjusting the stub spacing guides the center frequency wavelength. Fishtail stubs mitigate anti-phase magnetic currents, boosting microstrip line radiation. Circular polarization has been achieved with the help of phase difference and also, with the change in the location of feed point. It is appropriate for the mmWave N261 5G-band (27.5 to 28.35 GHz) because it covers 27.5 to 31 GHz. The MIMO antenna system uses these antenna pieces on 4 corners of a substrate. The authors propose a wideband CP MIMO mmWave design for 5G applications with a range of frequency from 27.5 to 31 GHz. The antenna is perfect for the millimeter wave N261 5G-band (27.5–28.35 GHz). The design is fed by a coaxial probe, eliminating complex feeding networks. To accomplish circular po-

TABLE 1. Comparison between the performances of slot and patch MIMO antennas.

Ref.	Shape of the Design/ Antenna/ Structure	Freq. (GHz)	Bandwidth (%)	Gain (dB)	No. of Elements	Efficiency (%)	ECC	MEG (dB)	DG (dB)	TARC (dB)	Isolation (dB)
[54]	Dual-mode slot-patch antenna	27	23	15.4 (array)	8	—	—	—	—	—	Ka-band
[53]	SIW triple-port annular slot antenna	27.5–28.05	0.55	8 (two-port)	—	88.78%	—	—	—	—	5G mmWave IBFD
[55]	Integrated MIMO antenna system	2.5, 3.5, 5.2, 24, 28	—	11.4 (28 GHz)	4 (millimeter-wave)	—	0.284	—	10 (over 2 bands)	—	− 22
[56]	Asymmetric flare-shaped patch MIMO antenna	20–40	10	8.17	2	—	< 0.0001	—	> − 20 (over 20–40 GHz)	> 20	Millimeter-wave communication
[57]	Tree-shaped planar quad element MIMO antenna	23–40	—	11.45 (38 GHz)	4	> 70%	—	< 3 dB	—	—	> 20
[58]	Wideband interconnected 3-element and 4-element MIMO design	26–40	43	—	3 (case 1), 4 (case 2)	> 20 dB (connected ground)	—	> 9.9	—	—	> 20
[59]	Compact-slotted four-element MIMO planar monopole antenna	27.1, 48.7	—	> 5.95	4	> 90%	—	—	—	—	> − 27
[60]	L-shaped microstrip line with fishtail stubs	27.5–31	—	—	4	—	—	—	—	—	—
[61]	Dual-band monopole components	27, 39	—	5.7 (39 GHz)	2	98.6% (39 GHz)	< 0.0001	10 dB	—	—	—

larization, the microstrip line is L-shaped with the feeding network moved from the corner.

In [61], two $26 \times 9 \times 11\,\text{mm}^2$ monopole components enable dual-band operation at 27 and 39 GHz. Investigation and optimization of mutual coupling minimizes the effect of one element on the other. The first and second bands of the MIMO antenna have 5 dBi and 5.7 dBi gains, respectively, and 99.5% and 98.6% radiation efficiencies. Tests of MIMO performance show a diversity increase of 10 dB over the two operational bands and an envelope correlation of 10–4. The design investigations in [61] are:

- The study explores novel frequencies in the MMW region using two wide bands.
- Thorough analysis of radiation and diversity performance.
- The design is Planar and easy-to-fabricate.
- High element isolation.
- Achieved high efficiency of radiation with the RT Rogers 5880 dielectric substrate.

Table 1 gives a detailed overview of millimeter-wave antenna designs, including key technical criteria for assessing their appropriateness for MIMO applications in mmWave communication systems. Operating frequencies, bandwidths, gains, elements, efficiency, and critical performance indicators classify designs. Also provide the insight about the following performance's parameters.

- ***The envelope correlation coefficient (ECC):*** measures the correlation between antenna element signals, a key statistic for MIMO system performance.

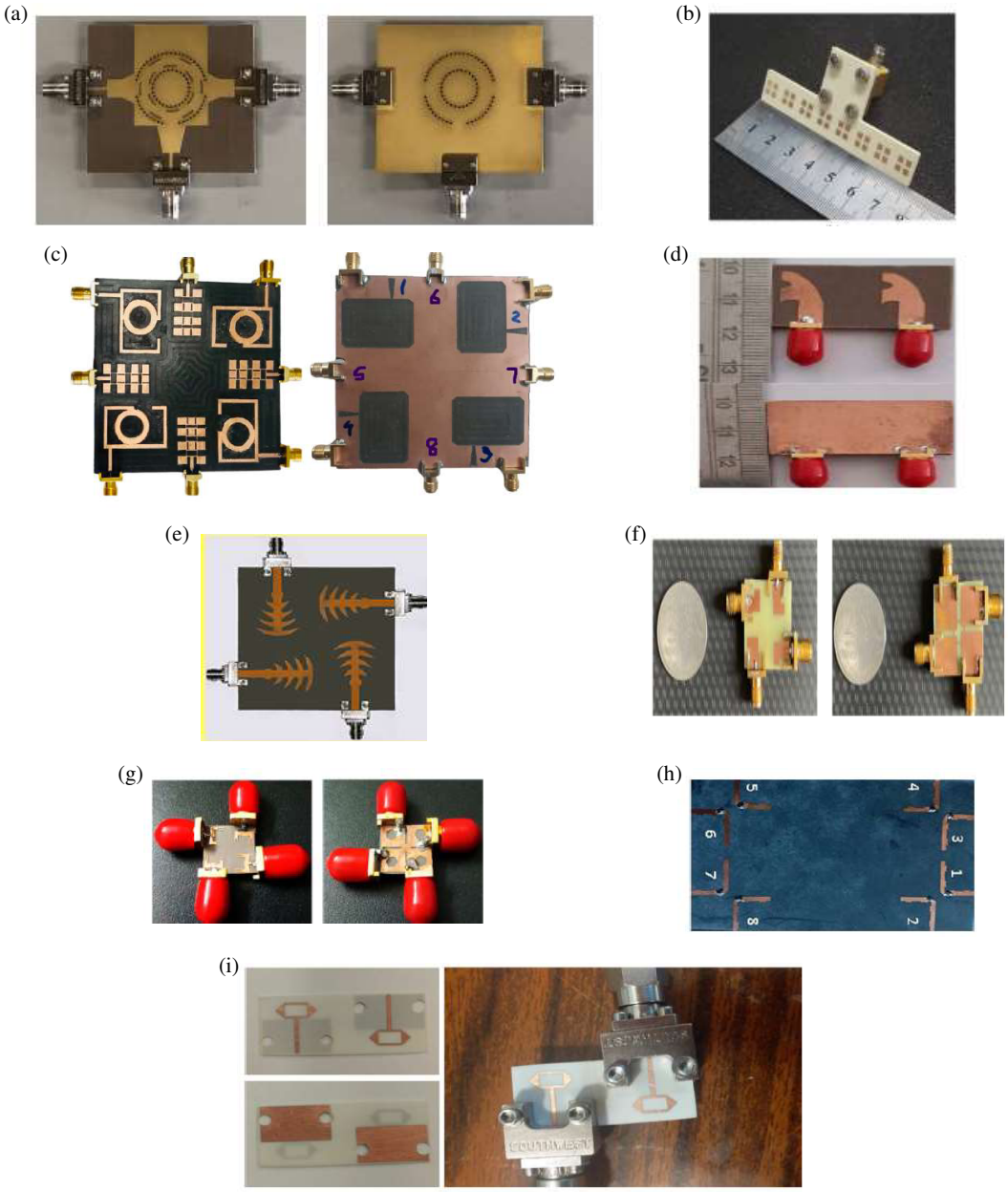

FIGURE 9. Fabricated slot/patch MIMO design, (a) [53], (b) [54], (c) [55], (d) [56], (e) [57], (f) [58], (g) [59], (h) [60], (i) [61].

- ***Channel Capacity Loss (CCL):*** Quantifies antenna correlation-induced channel capacity loss, revealing the system's transmission capability.
- ***Mean Effective Gain (MEG):*** The antenna's average gain across all signal directions, adding to the system's link budget.
- ***Diversity Gain (DG):*** Measures signal quality increase from many antennas, an important system reliability characteristic.
- ***Total Active Reflection Coefficient (TARC):*** calculates antenna element reflections, affecting signal integrity and system efficiency.
- The degree of separation between antenna elements reduces interference and improves MIMO system performance.
- Figs. 9(a)–(i) show antenna prototypes, revealing their physical designs. These extensive descriptions and performance measurements help researchers choose antennas for specific applications and optimize mmWave MIMO communication systems.

3.2. Defected Ground Plane MIMO Antennas

Millimeter-wave MIMO antennas benefit from deflected ground structures. To reduce antenna part interaction, the ground plane was artificially designed. In millimeter-wave MIMO systems with crucial antenna separation, DGS min-

imizes interference, improving signal quality and network stability. By decreasing mutual coupling, DGS allows small antennas to be placed near together without affecting performance. For 5G networks to deliver quicker data transfer and greater connectivity in densely populated locations, this technology is essential.

For 5G and Internet of Things (IoT) applications, a compact 2-band 2-element MIMO design is proposed in [62]. The antenna has the frequency of operation between 26.5 and 27.1 GHz and 39.15 and 40.69 GHz in millimeter wave (mmWave) frequencies. MIMO elements have a meandering patch and a ground plane with two symmetrical rectangular slots. The antenna has dimensions of $10 \times 28 \times 0.787\,\text{mm}^3$ and a maximum gain of 7.29 dBi at resonance frequencies of 26.8 and 39.8 GHz, respectively. Our antenna outperforms others due to its design compactness, low ECC (< 0.03) and isolation, superior gain, and efficiency. This study examines the antenna's CCL, MEG, and DG characteristics, which have not been studied in other antennas with similar applications.

A two-element arrangement actuated by a T-junction power combiner/divider feed network [63]. Although the ground plane is purposely modified with the help of different slot shapes like rectangular, circular, and zigzag, the array uses rectangular slotted-patch antennas. To improve antenna radiation, this alteration is made. To evaluate performance, the MIMO structure is built and measured. In [63], authors claim that structure can use 25.5–29.6 GHz for millimeter wave 5G applications. In the stated frequency range, the maximum gain is 8.3 dBi. To isolate antenna elements, polarization diversity is used between adjoining radiators, reducing Envelope Correlation Coefficient. Further performance indicators of the suggested structure include DG, CCL, and MEG.

According to [64], MIMO antennas have a rectangular patch structure with a 1×2 layout. Each patch is placed in the center of a $20 \times 20\,\text{mm}^2$ RO4350B substrate. Rectangular slots are added to the ground layer and radiating patches to downsize and improve performance. A center ground plane E-shaped slot is also appropriately placed. The antenna's operating impedance bandwidth covers the key mmWave frequency spectrum ranges from 26.4 to 30.9 GHz. MIMO antenna performance indicators include the ECC, which must be below 0.12 for each 2-element array to meet the standard of 0.5. It also has strong Diversity gain (DG), optimum at 10. The antenna has a minimum isolation of -19 dB and an efficiency of 85% at 28 GHz.

Sub-mmWave 5G New Radio (NR) n257/n258/n261 bands were covered by a compressed Coplanar Waveguide (CPW) fed linked ground MIMO antenna [65]. A compact structure with a wide working bandwidth, good gain & improved efficiency of radiation results from planar design. Top of antenna features modified CPW with two circular components feeding centrally slotted patch. Arranging the single antenna arrangement rotationally orthogonally creates a 4-port design. The bottom plane of the ground is connected by a circular ring for isolation levels > -20 dB across the band of frequency. The design of $24 \times 24\,\text{mm}^2$, the broad bandwidth ranges from 24.8–44.45 GHz (79.35%), 8.6 dBi is the maximum gain, and 85% of minimum efficiency are achieved by the authors.

This antenna has two mushroom-shaped radiating units and a ground plane with two square ring-loaded flaws [66]. A 43.17% impedance bandwidth of 31.6 GHz to 48.8 GHz was found in antenna research. With DGS, MIMO antennas exhibit low mutual coupling ($|S_{21}|, |S_{12}| < -20$) dB. Authors examine antenna performance aspects like return loss, radiation pattern, gain, and efficiency. For ultra-wide band (UWB) frequencies, diversity factors such as mutual coupling, ECC < 0.002, DG > 9.995, CCL < 0.3 bits/sec/Hz are achieved.

A circular microstrip patch antenna operates at 28 GHz, featuring a single element with an elliptical slot and an unconventional ground construction [67]. This MIMO antenna is $20 \times 20 \times 0.8\,\text{mm}^3$. With a bandwidth of 2.1 GHz, simulations show that the return loss at each port is less than -10 dB from 26.867 to 28.975 GHz. The antenna has 9.24 dB gain due to unidirectional emission and mutual coupling below -20 dB.

Small four-port uniplanar MIMO for n79/n46/mmWave applications is proposed in the paper. The quad MIMO design has dimensions of 30 by 30 by $0.8\,\text{mm}^3$. The MIMO design employs 4 Z-shaped radiators that are identical to one another and share ground on the same plane. Isolation barriers are not used. It has a bandwidth of 12 GHz and can cover frequencies between 18 and 30 GHz throughout the frequency ranges from 4.4 to 6.3 GHz, with a middle frequency of 5.6 GHz. The isolation for the mid-band was -11 dB, and the isolation for the mmWave was -24 dB. Good diversity performance can be achieved using uniplanar quad MIMO (DG $= 10$ dB, ECC 0.07, TARC -3 dB, MEG -5 dB, MEG $= 1$ dB). The impacts of the system hand specific absorption rate (SAR) were within acceptable parameters. Following an investigation of the micro quad MIMO design, simulations and evaluations of 8-port and 16-port uniplanar MIMO antennas were performed on dielectric substrates, the size of smart phones.

The Ultra-Wide Band (UWB) antenna in [69] uses Defective Ground Structure (DGS) technology from 25 to 50 GHz. The prototype may integrate many telecommunication devices for different applications due to its small size. The design dimensions are $33\,\text{mm} \times 33\,\text{mm} \times 0.233\,\text{mm}$. Second, element connections greatly impact MIMO antenna diversity. MIMO systems perform best in diversity due to orthogonally placed antenna elements. Also, align DGS and antenna elements for operating band separation. A DGS reduces mutual coupling and boosts gain to tune a reference antenna for bandwidth augmentation.

Table 2 provides an in-depth look at cutting-edge millimeter-wave antenna for a variety of uses. A variety of parameters, including ECC, CCL, MEG, DG, TARC, and Isolation, are shown for each entry, each of which is designated by a reference number. The advances in size, variety, and performance of these antennas make them ideal for use with cutting-edge wireless standards like 5G IoT, mmWave 5G, and UWB. Also, the design fabrications are shown in Figs. 10(a)–(g), and each unique layout, from winding grids to concentric rings to Z-shaped radiators, is tailored to meet a variety of communication requirements. To ensure optimal performance for diverse communication scenarios and developing technologies, this thorough description is a vital reference for engineers and academics.

TABLE 2. Comparison table of the performance of the defected ground structures MIMO antenna.

Ref.	Shape of the Design/ Antenna/ Structure	Freq. (GHz)	Bandwidth (%)	Gain (dB)	No. of Elements	Effiiency (%)	ECC	CCL	MEG (dB)	DG (dB)	TARC (dB)	Isolation (dB)
[62]	Meandering patch with slots and ground modification	26.5–27.1, 39.15–40.69	—	7.29, 7.45	2	—	—	—	—	—	—	—
[63]	Slotted-patch antennas with modified ground	25.5–29.6	—	8.3	2	—	< 0.03	—	—	> − 20	—	—
[64]	Rectangular patch with slots (1 × 2 configuration)	26.4–30.9	—	—	2	85%	< 0.12	—	10	—	− 19	—
[65]	Circular patch with CPW and circular structure	24.8–44.45	79.35	8.6	4	85%	—	—	—	—	> − 20	—
[66]	Mushroom-shaped radiating units with DGS	31.6–48.8	43.17	—	—	—	< 0.002	< 0.3	> 9.995	> − 20	—	<− 20
[67]	Circular microstrip patch with elliptical slot	26.867–28.975	2.1	9.24	1	—	< − 10	—	—	> − 20	—	>− 20
[68]	Z-shaped radiators with shared ground	4.4–6.3, 18–30	12	—	4	—	< 0.07	< − 3	< − 5, 1	10	—	− 11 (mid-band), − 24 (mmWave)
[69]	DGS technology with small form factor	25–50	UWB	—	—	—	—	—	—	—	—	—

3.3. MIMO Antenna Array

Advanced wireless communication technologies like MIMO array antennas are leading. Their ability to transmit and receive several data streams simultaneously improves data throughput and network efficiency. In millimeter-wave frequencies, where data transmission is rapid but sensitive to environmental influences, MIMO arrays improve reliability through spatial variety. MIMO technology, which uses multiple antennas, boosts data throughput and network coverage, ensuring connectivity even in highly populated urban areas. This game-changing capability makes MIMO array antennas essential for next-generation millimeter-wave networks' high-speed, low-latency communication.

According to [70], the antenna array dimensions are $1.02\lambda \times 3.86\lambda \times 0.021\lambda$ (at 25.66 GHz). Experimental results show a bandwidth of 49.62% (25.30 GHz to 42.0 GHz) with a 12.02 dBi of peak gain. In addition, the ECC is < 0.0014; the isolation between the design components is greater than 24 dB; and the channel capacity loss (CCL) is less than 0.29 bits per second per Hertz for the mmWave MIMO antenna array across the full frequency range. DGS-loaded mmWave modeling requires CPW feed, patch, and DGS. The whole antenna equivalent circuit is depicted in Fig. 11. Authors built, altered, and optimized an analogous circuit in AWRMicrowave Office ver. 22.1 for antenna design validation. Fig. 11 lists component values. Additionally, the design is suitable for future mmWave communication technologies, particularly 5G-enabled portable devices and base stations. These systems are expected to operate in frequency bands such as n257 (26.5–29.5 GHz), n260 (37.0–40.0 GHz), n261 (27.5–28.35 GHz), and other bands falling under frequency range 2 (FR2) established by the 5G new radio (NR) standards.

The antenna array contains four evenly spaced concentric pentagonal slots [71]. A single open-end microstrip transmission line excites the antenna in the sub-6 GHz range, while a 1×8 power divider (PD) with a T-junction construction excites the mmWave spectrum. The design was made on a $120 \times 60\,\text{mm}^2$ substrate with a 49 mm edge-to-edge spacing. The mmWave design operates at frequency band of 28 GHz (with at least 500 MHz bandwidth), whereas the sub-6 GHz antenna covers the frequencies of 4–4.5 GHz, 3.1–3.8 GHz, 2.48–2.9 GHz, 1.82–2.14 GHz, and 1.4–1.58 GHz A complete design study comprises a step-by-step design technique, diagram of equivalent circuit, and millimeter-wave and sub-6 GHz current density analysis, according to the authors. MIMO performance demonstrates that the suggested antenna design works effectively with a 0.113 maximum envelop correlation coefficient. Gain and efficiency peaked at 91% and 8.5 dBi across

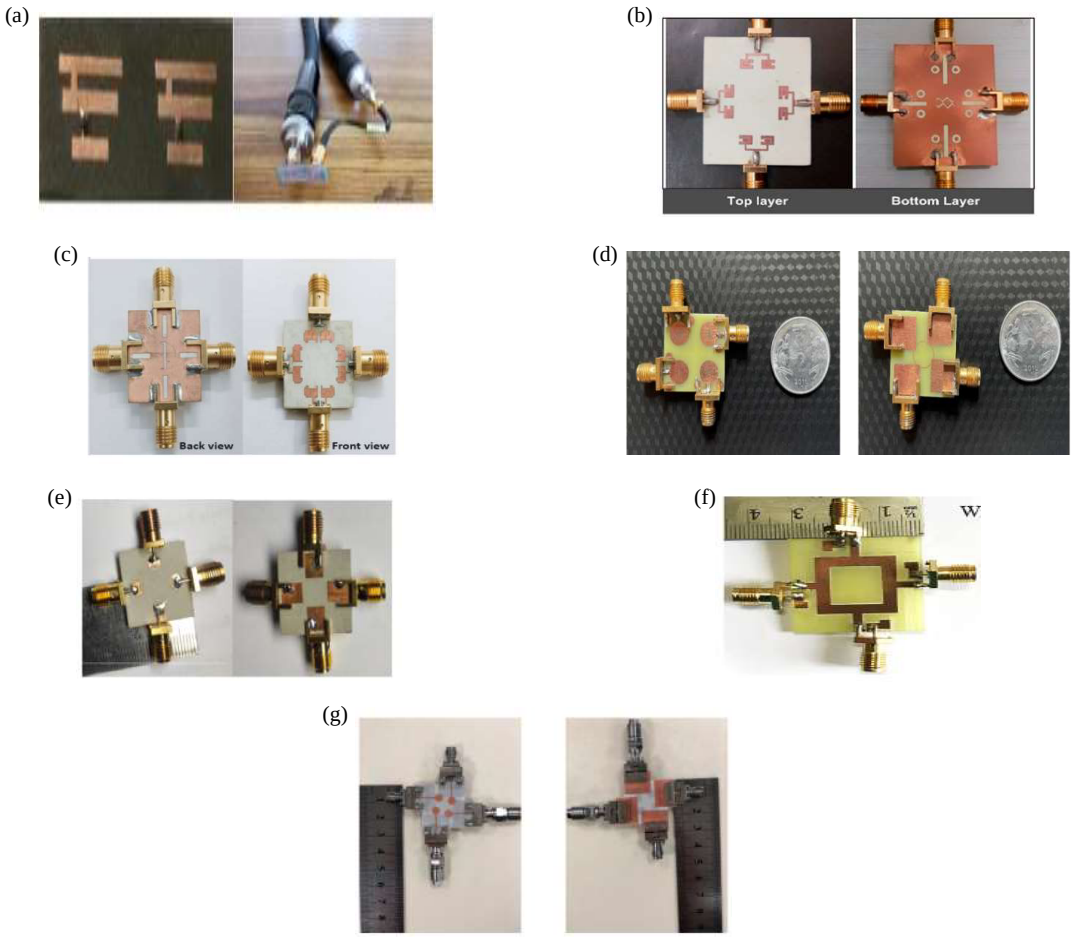

FIGURE 10. Fabricated defected ground plane MIMO design, (a) [62], (b) [63], (c) [64], (d) [65], (e) [67], (f) [68], (g) [69].

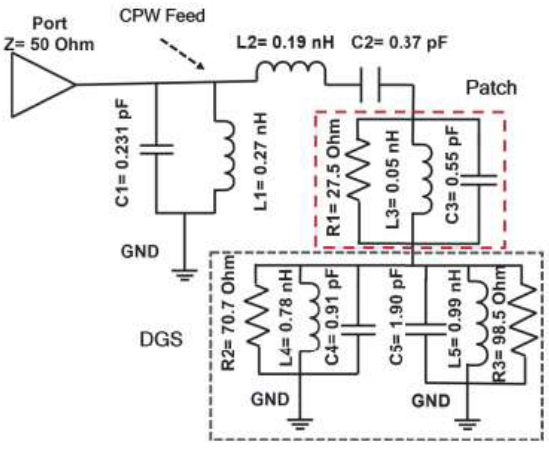

FIGURE 11. Equivalent model [70].

the complete operation band. The design supports 4G and future 5G wireless communication systems, including sub-6 GHz and 28 GHz bands.

This study presents a 2-element MIMO antenna for 5G enabled access points employing the same components in sub-6 GHz and millimeter-wave bands with different feeding topologies. The contributions of the work include:

- The antenna design emphasizes the utilization of millimeter-wave antennas in conjunction with sub-6 GHz antennas that share the same radiating aperture/structure.
- The research presents a novel concept for a 5G access point that makes use of a shared aperture antenna architecture that operates at sub-6 GHz and millimeter-wave frequencies and has pentagonal slots. Because of this, distinct antenna structures for millimeter-wave frequencies and sub-6-gigahertz bands are no longer necessary.
- A design for a multi-band antenna incorporates basic modes for each circular slot. Better gains and efficiency values in all major modes make the antenna an attractive option.
- The antenna that was recommended demonstrates outstanding MIMO performance in both the sub-6 GHz and the 28 GHz millimeter-wave bands.

The suggested concept uses a co-shared radiating design for both sub-6 GHz and mmWave bands, despite their unique feeding mechanisms. This is a unique feature of the antenna design [71]. Moreover, the operation of a 6-band MIMO design for sub-6 GHz and mmWave bands has never been reported before as claimed by authors.

A 2×2 microstrip antenna array of $11.9 \times 15.3\,\text{mm}^2$ and operating at 38 GHz is described in [72]. Design achieves

14.58 dB gain, −17.7 dB return loss, and 500 MHz impedance bandwidth. Duplicating this antenna twelve times at 30° creates a dodecagon with low-profile. Each sector can cover 58° for 12 (360-degree beams). Our antenna concept was smaller and had more gain than published antennas targeting compact size and low profile at 38 GHz.

The tapered slot antenna (TSA) array has been designed for mmWave massive multi-beam communication [73]. The authors claim that element spacing matching half-wavelength requirements in the H-plane allows the antenna array to perform well in beam-forming. Millimeter-wave electronics can directly integrate with the design element via a SIW. Reflection coefficient < -15 dB, VSWR < 1.45 in 22.5–32 GHz range, meeting ITU 24.25–27.5-GHz and FCC 27.5–28.35-GHz 5G requirements. The antenna element's 24–32 GHz gain is 8.2–9.6 dBi. Medium gain and big bandwidth make the TSA appropriate for mmWave communication systems. This antenna can form a half-wavelength H-plane array. A SIW-fed metallic TSA with a distinctive tapered slot transition forms the antenna element. The design's impedance matching and emission patterns are excellent across many frequencies. The SIW feeding topology simplifies antenna array integration with planar circuitry.

[74] describes MIMO antenna array elements as triplet circular rings with an infinite shell. The design's simulated gain was 6.1 dBi, while the gain was 5.5. Additionally, actual and simulated antenna efficiency are 90% and 92%. ECC for MIMO is below 0.16 throughout the whole operational bandwidth. The antenna features 16 dB isolation, 80% efficiency, and 2.45 GHz and 28 GHz frequency response. The described multi-band antenna design becomes more complicated with a tapered slot. Studies show that mmWave resonating structures are complex and huge. Due to the congested sub-6 GHz spectrum, mmWave offers a wide bandwidth to use for 5G's faster data throughput and reduced latency than 4G. The unique mmWave antenna's circular ring-shaped radiating construction provides high isolation without DGS, tapered slot, or EBG structures.

MIMO antennas are 2-element arrays which corporate feeding networks, while the single patch antenna with bow-tie slots and slits is designed by [75]. Vertical and horizontal slots serve as Defected Ground Structures (DGS) to improve antenna performance. The top surface has a decoupling structure (slotted zig-zag) carved from edge to edge for isolation. Spatial and polarization diversity isolate antenna elements (< -40 dB). The proposed antenna may provide 12.02 dBi gain in the 5G mmWave frequency with a −10 dB bandwidth from 27.6 to 28.6 GHz. A 2-element array with the DGS achieves high gain. A slotted construction reduces antenna interaction. The authors advised 5G connectivity research to focus on ultra-wideband operational frequency and mmWave channels. For wider coverage, add beam guiding. To span maximum 5G frequency ranges, shared aperture designs may include sub-6 GHz channels with millimeter Wave bands.

By the Rogers RT Duroid 5880 substrate, a single-element, $2:1$ VSWR array antenna is built for 5G applications in the 27.06–28.35 GHz frequency range [76]. The substrate measures $51.44 \times 18.34\,\text{mm}^2$. Each patch is approximately $3.8 \times 4.5\,\text{mm}^2$. The recommended array has a gain of 16.07 dBi, radiation efficiency of 93.5%. MEG for Gaussian medium is -9.85 to -13.05 dB with XPR $= 0$ dB and -7.50 to -10.71 with 6.0. Parallel port radiators with 45° corner chopping lower S parameter (return loss). In frequency band, the array antenna has over 16.07 dBi gain.

The proposed MIMO system has two antennas. Four elements are uniformly distributed in each antenna array, whereas two have a 90-degree tilt. The 37 GHz MIMO antenna array addresses 5G millimeter-wave communication. A four-element array can boost the antenna element's 6.84 dB gain to 12.8 dB. ECC and DG are below the standard for antenna array performance. The suggested MIMO antenna array has over 85% radiation efficiency in the defined operating frequency range.

Article [78] describes a redesigned circular patch radiating element for 2×2 5G MIMO arrays. Orthogonal radiating elements limit mutual interaction and boost system performance in the array. At a frequency of 28 GHz, the gain of 7.2 dBi and inter radiator isolation of about 26 dB are achieved by MIMO array. Each antenna has a measured 1.6 GHz bandwidth ranging from the 27.25 to 28.85 GHz. Also, the Frequency Selective Surface (FSS) boosts MIMO design gain to 8.6 dBi at 28 GHz. MIMO array radiation is perpendicular to its plain. 5G operational frequency (28 GHz, 26.5 GHz to 29.5 GHz) has an ECC < 0.002 and a DG of better than 9.99 dB due to low coupling between radiating elements in the MIMO design.

A MIMO-array beamforming antenna with a $2:1$ VSWR is designed for the band of 28.0 GHz in [79]. This antenna covers the frequency range of 27.04 to 28.35 GHz, making it suitable for the use in the mmWave n261 5G-band. A beamforming MIMO antenna typically has between one hundred and two hundred main lobe directions. Less than 28.0 dB of mutual coupling can be found between the MIMO-array ports. Both the gain and radiation efficiency in the band that was displayed are higher than 13.99 dBi and 93.0%, respectively. The proposed architecture benefits from a $\leq 10^{-4}$ ECC in the stated frequency spectrum. With 1.31 GHz of TARC active bandwidth, it is capable of supporting Gaussian applications both indoors and outdoors. It has simulated and measured fractional bandwidths of 4.65% and 4.73%, respectively. In order to minimize return loss, port radiators are parallel and have 450-degree cutting at the patch corners.

Table 3 summarizes various MIMO antenna arrays. These antenna array are tuned to certain frequency ranges, making them ideal for use with 5G networks. Their gains are substantial; their correlation coefficients are low; and their radiation patterns are effective. The designs incorporate cutting-edge features like circular rings, bow-tie holes, and orthogonal parts to guarantee top performance and compatibility with 5G technology requirements. Also, the design fabrications are shown in Figs. 12(a)–(j).

3.4. Dielectric Resonator Antennas (DRAs)

The effective methods for manipulating the circuit and radiation properties of DRAs are discussed [80]. In this section, the benefits of DRAs are detailed, along with the most effective antenna feeding and size reduction approaches. Additionally, advanced

TABLE 3. Comparison of the performance of MIMO design.

Ref.	Prototype	Freq. (GHz)	BW (%)	Gain (dBi)	No. of Elements	Effi. (%)	ECC	CCL	DG	TARC	Isolation (dB)
[70]	DGS-Loaded MIMO Array	25.3–42	49.62	12.02	2	—	< 0.0014	< 0.29	—	—	> 24
[71]	Concentric Pentagonal Slots	1.4–4.5, 28	4–4.5, 3.1–3.8, 2.48–2.9, 1.82–2.14, 1.4–1.58	8.5	1 × 8	—	Sub-6 GHz & 28 GHz MIMO	< 0.113	8.5	> 9.99	—
[72]	12-Element Dodecagon Array	38	500 MHz	14.58	2 × 2	—	—	—	—	—	—
[73]	Metallic Tapered Slot Array	22.5–32	ITU 24.25–27.5 GHz, FCC 27.5–28.35 GHz	8.2–9.6	—	8.2–9.6	Millimeter wave	—	—	—	—
[74]	Triplet Circular Rings	2.45, 28	Dual-Band	5.5	—	90–92%	< 0.16	—	—	—	16
[75]	Patch with Bow-Tie Slot and Slits	27.6–28.6	− 10 dB BW	12.02	2	—	—	—	> 9.99	—	> − 40
[76]	Circular Patch Radiating Element	27.06–28.35	-	16.07	2	93.50%	—	—	—	—	—
[77]	Orthogonal Radiating Elements	27.25–28.85	1.6 GHz	7.2–8.6	2 × 2	> 26 dB	< 0.002	> 9.99	—	—	—
[78]	MIMO-Array Beamforming Antenna	27.04–28.35	1.31 GHz	13.99	2 × 12	—	$\leq 10^{-4}$	—	—	> 93%	> − 28
[79]	2 × 2 MIMO Array	27.5–28.35	4.73%	> 13.99	2 × 2	—	$\leq 10^{-4}$	—	—	> 93%	> − 28

design methods to improve individual DRA gains are examined. Radio frequency (RF) front-end designers receive help on selecting antenna topologies to meet desired performance in frequency response, gain, and polarization. This section focuses on analyzing the development in applying DRA technology at millimeter wave frequencies.

Here are the primary benefits of DRAs:

- The size of the DRA is proportional to $\lambda_0/\sqrt{\epsilon_r}$, (where $\lambda_0 = c/f_0$ is the wavelength in free space at the (f_0) resonant frequency and ϵ_r is the relative permittivity). DRAs have a smaller form factor compared to typical metallic antennas, particularly when they are constructed out of materials that have a high dielectric constant (ϵ_r).

- Due to the absence of any substance that conducts electricity, DRAs that make use of low-loss dielectric materials demonstrate a high degree of radiation efficiency. Due to these properties, they are ideally suited for use in applications involving high frequencies, ranging from 30 GHz to 300 GHz. Also, conductor losses in common metallic antennas are increased when operating at these frequencies.

- A large impedance bandwidth for DRAs may be achieved by carefully selecting the size of the resonator and also the material's dielectric constant.

- DRAs can be excited using a range of different methods, which is beneficial for a variety of applications as well as integration of the array.

3.4.1. Millimeter-Wave DRAs

Inherently, DRAs have no conduction losses, which makes DRAs useful for the applications of high-frequency. Technology of DRA at millimeter wave frequencies has advanced recently. mmWave frequencies and beyond require small DRA, making DRA manufacturing problematic without expensive fabrication. Electrically larger DRAs with higher-order modes can overcome this limitation and boost antenna gain. For better antenna gain and broadband performance the combination circular patch and ring-shaped DRA are used in [81]. Radiating structures have a 12% impedance matching bandwidth (57 GHz–64 GHz) according to numerical predictions. Simulated antenna gain is 16.5 dBi, the highest for a single-element DRA. [82] describes substrate integrated waveguide-fed cylindrical DRAs with linear and circular polarization. The DRAs

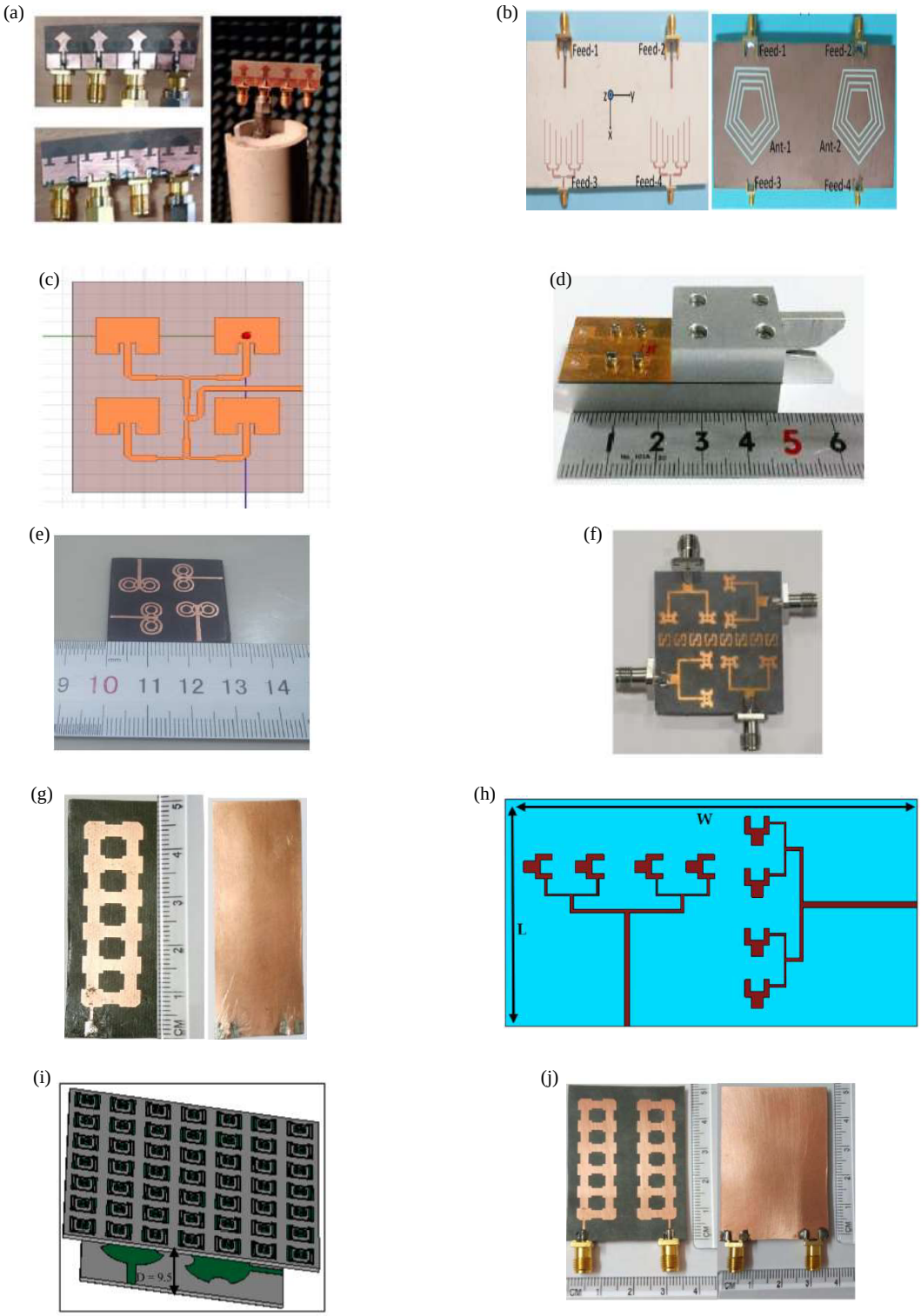

FIGURE 12. Fabricated MIMO array design, (a) [70], (b) [71], (c) [72], (d) [73], (e) [74], (f) [75], (g) [76], (h) [77], (i) [78], (j) [79].

are 60 GHz resonance-oriented. Linearly and circularly polarized DRAs have 24% and 4.5% impedance bandwidths, respectively.

Bond-wiring is reduced by direct antenna integration on chip, enabling downsizing and lower manufacturing costs. The 60 GHz (rectangular) and 27 GHz (Circular) DRA on the substrate of silicon is described in [83, 84]. Setting the dielectric resonator's relative permittivity higher than the silicon substrate's ($\epsilon_r = 11.9$) decreases fringing field effect and substrate losses by concentrating RF power on it. When DR permittivity

TABLE 4. Comparison performance of millimeter wave DRAs.

Ref.	Type of DRA	Frequency in GHz	Bandwidth in %	Gain in dB	Gain Enhancement Method	Efficiency in %	Mode
[85]	Hemispherical	25	35.8	9.5	3 layer DRA	90	TE711
[86]	Cylindrical	20	75.8	5.65	Hybrid Multi-permittivity DRA	92	HE11
[87]	Cylindrical	30	16.6	11.3	conical horn (Truncated Plastic based)	94	HE11
[89]	Rectangular	35	12	5.5	substrate-integrated dielectric resonator antenna	94	TE10

TABLE 5. Comparison performance of DRAs array.

Ref.	Type of DRA	Frequency in GHz	Bandwidth in %	Gain in dB	No. of element	Efficiency in %	Mode
[91]	Rectangular	34	4.7	11.7	4	90	TE10
[92]	Rectangular	35	6.4	21.5	64	85	TE111
[93]	Rectangular	38	2.5	13	12	91	TE11δ
[94]	Grid	32	18.4	12	8	76	TE10
[96]	Rectangular	28	31.6	8	4	86	TE3δ1

is $40 < \epsilon_r < 70$, antenna gain and radiation efficiency show better performance, according to research. A 45% efficiency and 1 dBi gain of cylindrical DRA on silicon substrate is given in [68], while a rectangular DRA is presented in [83]. Isolating the DR from the lossy substrate & directing the radiation beam broadside gives the antenna with CPW feeding mechanism 3.2 dBi gain at 60 GHz.

[85] presents a three-layer mmWave hemispherical DRA with 35.8% impedance bandwidth, 9.5 dBi maximum gain, and 90% radiation efficiency. Assembling the three dielectric layers is difficult and expensive with this technology. Antenna air gaps boost multilayer DRA gain [86]. For mmWave applications, this study used a DRA (low-profile hybrid multi-permittivity) with perforated construction. Drilling the DRA increases bandwidth by creating air holes. Small DRAs make it hard to maintain air hole size and distance. Authors made 21 identical cylindrical holes in the dielectric resonator. While retaining 5.65 dBi gain, operational bandwidth increased 27.4% from 48.4% to 75.8%. An similar mmWave approach utilizes a DRA with a conical horn (plastic-based) to boost gain [87]. A slot-coupled microstrip line drove the antenna, which had 16.6% bandwidth, 94% radiation efficiency, and 11.3 dBi gain. DRA gain is 8 dBi without the plastic conical horn. However, antenna placement is tricky. Surface-integrated waveguide (SIW) technique maximizes DRA gain and efficiency [88].

For millimeter-wave applications, [89, 90] discuss DRA properties including feeding, reduction of size, and gain improvement to help designers of RF front-end to choose antenna designs for gain, optimal response of frequency and polarization and the Table 4 compares millimeter wave DRA performance.

3.4.2. Dielectric Resonator Antennas Array

Many factors have been used to improve DRA array gain in various studies. Specific references [91–94] used SIW feed networks. Wahab et al. [91] used N-element array of linear elements and 2-feeding slot configurations to improve radiation efficiency. A study by the same authors as [91, 95] employed a SIW feeding network at a frequency of 33.9 GHz to build a four-DRA array with 11.70 dBi gain, 4.7% bandwidth, and 90% efficiency. Absence of matching circuit to promote coupling in SIW longitudinal slot situation is a drawback of [91].

Four DRA elements of connected rectangular ring at a frequency of 28 GHz are proposed in [96], employing glue to shrink air gaps between the ground plane and DRAs. To improve alignment, dielectric structure contains arms. However, dielectric arm positions greatly affect DRA mutual coupling, radiation efficiency, and gain. Table 5 compares mmWave array linear polarized DRA performance.

Mutual coupling between MIMO elements can substantially reduce MIMO system performance and antenna characteristics. Thus, metamaterial walls have been used to reduce MIMO element mutual coupling [97, 98], which greatly reduced mutual coupling.

In [99], metallic vias are used to decouple millimeter-wave MIMO dielectric resonator antenna units for better isolation. At appropriate locations, DRA pieces have vertical vias. Vias

FIGURE 13. Fabricated DRA array antennas, (a) [99], (b) [100].

interact with electromagnetic fields to affect field distributions and lower linked fields. DRA of MIMO elements can be better isolated. The vias in the DRA components make the antenna system small and straightforward. The feasibility and universality of this technology were demonstrated by developing, constructing, and measuring two examples: an H-plane and an E-plane connected 1×2 MIMO DRA arrays. Using vias efficiently can isolate the H-plane connected MIMO DRA array and the E-plane array are from 15.2 to 34.2 dB and from 13.1 to 43 dB respectively at 26 GHz. For the first time in [99], advocates employing simple metallic vias to isolate mmWave MIMO DRA parts. Research shows that vertically placing vias inside DRA elements reduces mutual coupling without increasing antenna footprint or height. Although the decoupling vias change the excited antenna's field distributions, the emission patterns are essentially identical to the single DRA. Since the DRs are the principal radiator and the vias do not resonate in the operational band, their loss is negligible.

In [100], rectangular microstrip-fed slots activate the substrate using dielectric resonators (DRs). To isolate antenna elements, each DR includes an upper metal strip that redirects the strongest coupling field from the exciting slot. The design has a frequency spans of 27.5–28.35 GHz at the 28 GHz and gives the isolation of 12 dB. For the boosting of isolation, a metal strip on the upper side of each DR is placed. The proposed MIMO DRA with metal strips has no DRA impedance matching difficulties and a reflection coefficient of less than -10 dB at 27.25–28.59 GHz. Fig. 13 depicts the prototype.

In [101], a rectangular DRA with four elements is proposed for 5G applications, having slot-coupled microstrip feeds for each element. The size is of the design 20 mm $\times$ 40 mm. Four DRAs are placed above the slot with precision. Metamaterial is printed on top of the DRA to improve the isolation by removing solid coupling fields. Interaction between metamaterial structure and electromagnetic fields disrupts field distributions, reducing coupled fields. The structure operates at 2.23 GHz, covering the 28 GHz, ranging from 27.5 GHz to 28.35 GHz, FCC-allocated spectrum for 5G applications. It operates from 26.71 GHz to 28.91 GHz. The suggested structure exhibits broadside radiation with gain exceeding 7 dBi across all working bands with all four-port stimulation. Also, the fabricated prototype is given in Fig. 13.

3.4.3. Circularly Polarized Dielectric Resonator Antenna

Different dielectric materials are used for feed structure and DRA. DRA installation errors on the feed network can severely damage antenna performance. This is especially true for millimeter-wave operations. The integrated DRA substrate idea uses the same material and production technique for the 4-Dielectric Resonators elements and feed network, eliminating errors. This design had 1.6% bandwidth and 13.6 dBi linear polarization gain. Moreover, the axial ratio bandwidth of 1.1%, the CP antenna offers 16.48% bandwidth and 12.7 dBi gain. The element's profile, which limits [102], was ignored.

5G mmWave applications use a unique single-fed Dielectric Resonator Antenna (DRA) [103]. In 5G channels, the DRA achieves dual bandwidths and circular polarization. This two band antenna resonates at 22.06, 24.5, and 29.84 GHz. The bandwidth ranges 19.52–26.36 GHz and 7.69% at 28.26–30.26 GHz. Both obtained bands are 5G Band 30 GHz. A 50 Ohm microstrip line feeds a trapezoidal DRA instead of a rectangular one. The DRA has electrical dimensions of $0.25\lambda_0 \times 0.29\lambda_0 \times 0.22\lambda_0$ and a resonating frequency of 26 GHz. DRA is mounted on a RT duroid substrate ($0.5\lambda_0 \times 0.5\lambda_0 \times 0.1\lambda_0$) with a permittivity of 2.2. DRA is circularly polarized and has 5.23% axial ratio bandwidth of 3 dB. DRA gain 3.28 dB. Circularly polarized wideband antenna with enhanced signal-to-noise ratio is reported in [103]. The design is circularly polarized using the microstrip line (edge feed) to the DRA. Various feeding sites are evaluated for circular polarization using edge feeding.

At 26 GHz, a trapezoid DRA achieved 26.3% bandwidth and 5.2% axial ratio [104]. However, angular cutting of the rectangular DRA framework into a trapezoid may have caused production errors. In [105], a coaxial probe stimulated and drilled a cylindrical DRA at 26 GHz. This method is difficult and rarely used in investigations. High tolerance is needed for fabrication. Metasurface converts linear polarization to circular polarization. The metasurface boosts gain and axial ratio. Circular polarized bandwidth of 26.3% and axial ratio of 1.35% are achieved. In [106], a SIW-stimulated DRA (stacked rectangular structure) has been used at 20 and 30 GHz. Two rectangular DRAs are stacked with a metal strip on top to get circular polarization in both frequency bands. However, its many steps and components make this procedure complicated and expensive. At 20 and 30 GHz, circularly polarized bandwidths of 6.4% and 12.8%, with axial ratios of 5.2% and 4.1% have been featured. Despite its complexity, this study did not address alignment. Also, Table 6 compares the performance of circularly polarized DRAs.

TABLE 6. Comparison performances of circularly polarized DRAs.

Ref.	Type of DRA	Frequency in GHz	Bandwidth in %	Gain in dB	Axial Ratio in %	Mode
[102]	Rectangular	30	16.48	12.7	1.1	TE11δ
[103]	—	28.26–30.26 GHz	—	—	—	—
[104]	Trapezoidal	26	26.3	3.28	5.28	TEx21
[105]	Cylindrical	26	26	6.6	1.35	TE412
[106]	Rectangular	30/30	6.4/12.8	6.6/8.2	5.2/4.1	TE111

Antenna designers can modify DRA circuital properties and radiation patterns at mmWave frequencies [107]. Many feeding systems and their benefits and cons are covered in [107]. Resonance at specific frequencies increases DRA gain. For higher-order modes, use larger antennas or horns. Circularly polarized DRAs can solve attenuation difficulties; however, there are few investigations on their application in the mmWave range. Numerous studies have examined MIMO methods. MIMO channel capacity, data throughput, compact size, and connection reliability can be improved by moving DRAs. Advanced DRA technology will make these antennas practical for real-world applications, surpassing popular ones.

3.5. Metamaterial/Metasurface Structures

A "metasurface" is a man-made structure with extraordinary electromagnetic properties including negative permittivity and permeability. In recent years, metamaterials and metasurfaces have garnered interest for their unique properties. These two materials appear to be capable technologies for enhancing microwave component performance and overcoming restrictions, particularly in antennas [108].

A new $30 \times 30 \times 1.52\,\text{mm}^3$ two band 28/38 GHz, 2×2 PCB-based, MIMO design with complementary Split Ring Resonator (CSRR) construction is shown in [109]. The antenna's gain and directivity are improved by placing CSRR metamaterial unit cells on top and ground. The comparison of actual and calculated results showed that the enhanced MIMO antenna array had a 28.29 GHz resonance frequency and -20.54 dB effective reflection coefficient at 38.78 GHz. They have 15.30% and 13.97% bandwidth and -24 dB and -38.71 dB isolation in their resonant bands. The realized gain is 8.65 dBi at 28 GHz and 8.24 at 38 GHz. ECC between MIMO antenna elements is 0.0041.

A 14 mm $\times$ 14 mm planar four-port microstrip line-fed MIMO antenna is introduced in [110]. The antenna operates at 28 GHz/38 GHz, possible 5G millimeter-wave frequencies. Rectangular patch antennas are used as primary radiators to achieve the resonant frequency of 28 GHz. Etching an SRR (single element) metamaterial unit cell formed from the fundamental patch radiator creates a 38 GHz resonance band. Port isolation between antenna elements exceeds 25 dB throughout both frequency bands without complex decoupling methods. Lumped components of the antenna's equivalent circuit diagram characterize its electrical responses. The diversity performance metrics studied were ECC $<$ 0.005, DG of 10 dB, and CCL $<$ 0.35 bits per second per hertz. The antenna described has numerous important qualities that makes a good candidate for the 5G RF antenna system. Additionally, the equivalent circuit model evaluates a system's electrical characteristics in relation to an RF signal input.

- The utilization of planar geometry, a straightforward design, and a convenient fabrication process are desirable attributes.
- The incorporation of a compact form factor is advantageous for seamless integration within 5G devices.
- Achieving high isolation between antenna elements without the need for elaborate decoupling structures.
- The practice of printing on a common ground plane is often exploited in [111].

In [112], a metamaterial-based two-band MIMO antenna ($5.5 \times 5.4 \times 0.508\,\text{mm}^3$) is reported for the 5G mmWave communication networks with high isolation. Two-band response and wide operating bandwidth are offered by the 5G 28/28 band pentagon-shaped monopole antenna. Two nearby symmetric radiating elements constitute the MIMO system, which has -18.5 dB mutual coupling at both of the frequency. Two radiators are separated by a dual-band metamaterial to reduce interaction. Adding a 3×1 metamaterial antenna array improves isolation to -39 dB at 28 GHz and -38 dB at 38 GHz. The system boasts a wide bandwidth, low profile, strong gain ($>$ 5 dB), enhanced isolation (-38 dB), low ECC ($<$ 0.0001), CCL ($<$ 0.05), and DG ($>$ 9.99 dB). It works on all 28/28 5G bands with excellent diversity performance, say authors:

Metamaterial-based MIMO was highly diverse. The 5G millimeter-wave communications system is stable with appropriate ECC ($<$ 0.0001), TARC ($<$ -10 dB), CCL ($<$ 0.05), and DG ($\approx$ 10 dB) values at 28/38 GHz dual-bands.

For 5G mm-Wave communication systems, [113] introduces a 4-element MIMO antenna with a 1×2 metasurface design and corporate feed parallel network. Furthermore, a 9×6 CSR metasurface array improves MIMO antenna gain and isolation. In mmWave frequency, the antenna operates from 24.55 to 26.5 GHz. After adding the metasurface layer, peak gain was 10.27 dBi. Metasurface boosts isolation by 5 dB. MIMO performance measures including ECC, DG, CCL, and MEG demonstrate good antenna characteristics. The metasurface of 9×6 Circular Split Ring (CSR) cells on MIMO antennas enhances gain and reduces coupling effects.

In [114], the design has a patch with truncated corner and a 2×2 periodic square metallic plate metasurface. The antenna's

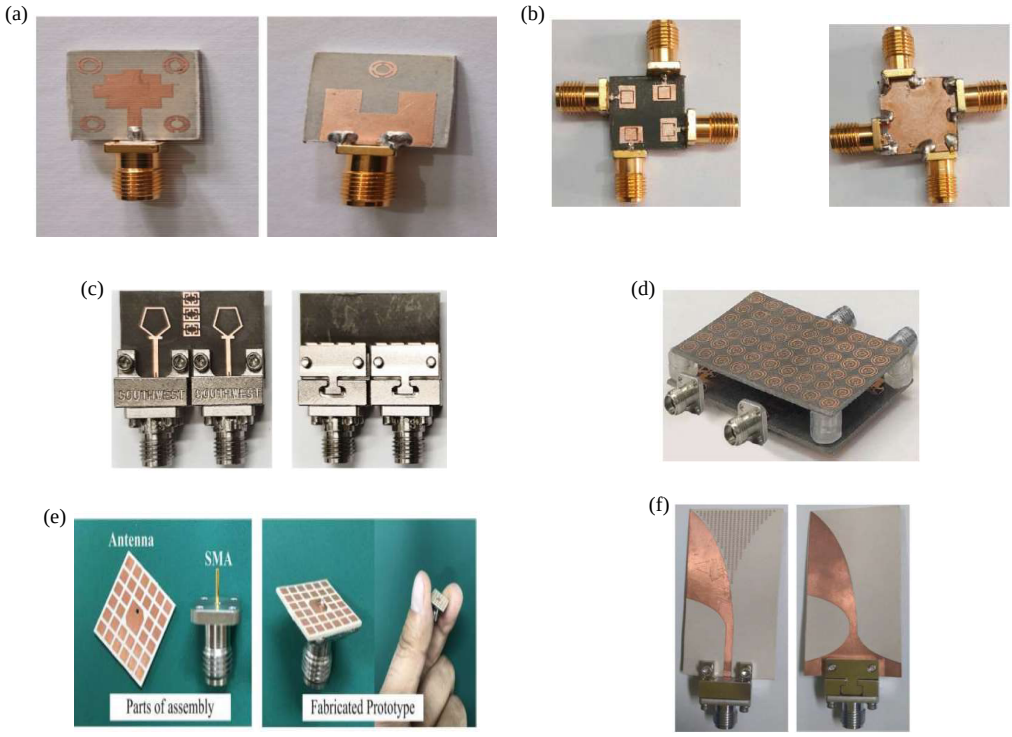

FIGURE 14. Fabricated metamaterial inspired antennas, (a) [109], (b) [110], (c) [112], (d) [113], (e) [114], (f) [115].

low profile, low cost, high gain, and wideband features are obtained by printing all radiating parts (radiator and MS) on the dielectric substrate's single layer. Wideband CP radiations from the MS's surface-waves are detailed. The small single-layer antenna is $1.0\lambda_0 \times 1.0\lambda_0 \times 0.04\lambda_0$. Simulations and experiments show that metasurface design has a broad 10 dB impedance bandwidth of 23.4% and an overlapping 3-dB axial ratio bandwidth of 16.8%. Stable radiation patterns, $>$ 95% radiation efficiency, and 11 dBic flat gain characterize the antenna. Additionally, a 4-port (2×2) MIMO is designed with perpendicular parts. Without decoupling, MIMO antennas perform well in isolation, envelope correlation coefficient, and channel capacity loss. Mainly, the antenna operates in the 5G mmWave range from 25–29.5 GHz. Key author contribution [114]:

• The authors present a single-layer planar antenna with CP and MIMO capabilities for the 25–29.5 GHz 5G band with a low height profile (0.51 mm) and few assembly elements, making it cost-effective and mass-manufacturing

A wideband antipodal Vivaldi antenna (AVA) with a negative index metamaterial (NIM) was designed in [115]. The antenna is linearly tapered. Negative index metamaterials improve antenna performance. The top surface between two AVA radiators has 'V'-shaped metamaterial unit cells that increase the end-fire electric field. The antenna having a size (50 mm $\times$ 24 mm $\times$ 0.51 mm) is small compared to other AVA antennas. The antenna can acquire 15.26 dBi at 41.3 GHz. The gain is relatively stable, ranging 9.25 ± 1.75 dBi at 15–40 GHz. No high-gain millimeter wave antenna is available, according to the authors. But also, various techniques are found in the literature to improve the performance of the antennas at millimeter wave [116, 117].

Table 7 lists 5G MIMO antennas' frequency bands, diameters, bandwidths, gains, isolations, and performance metrics like ECC, CCL, MEG, and DG. Figs. 14(a)–(f) show the Metamaterial Inspired antenna.

4. TECHNICAL CHALLENGES, SCIENTIFIC AND TECHNOLOGICAL TRENDS: IN MILLIMETER WAVE ANTENNAS

- ***Beam Steering Techniques:*** Achieving beam steering capability is vital for 5G applications. The review suggests the utilization of RF p-i-n diodes, phase shift techniques, or beam switchable technologies. However, improvements are needed, especially in adapting beam steering techniques for handheld devices in addition to base stations.
- ***Compact Design for Diversity Parameters:*** Future MIMO designs should prioritize compactness to meet diversity parameters efficiently. Compact antennas capable of maintaining consistent performance across different frequencies are essential for overcoming challenges in 5G deployment.
- ***Frequency Range and Amplification:*** Millimeter-wave MIMO antennas for 5G must operate effectively across a broad frequency range. Achieving substantial amplification while maintaining consistent voltage levels across all ports is a significant challenge that needs attention for seamless 5G implementation.

TABLE 7. Comparison of the performances of circularly polarized DRAs.

Ref.	Design	Freq. Bands in GHz	Antenna Size (mm)	Bandwidth in %	Peak Gain in dBi	Isolation (dB)	ECC	CCL (bits/s/Hz)	MEG (dB)	DG (dB)	TARC (dB)
[107]	CSRR-Enhanced MIMO Array	28, 38	30 × 30 × 1.52	15.30, 13.97	8.65, 8.24	−24, −38.71	0	—	—	—	—
[109]	Planar Microstrip MIMO	28, 38	14 × 14	—	—	> 25	< 0.005	< 0.35	—	> 10	—
[110]	Metamaterial-Based Dual-Band MIMO	28, 38	5.5 × 5.4 × 0.508	—	> 5	−18.5, −38	< 0.0001	< 0.05	> 10	> 9.99	< −10
[111]	Metasurface-Based MIMO	24.55–26.5	—	—	10.27	—	—	—	—	—	—
[112]	Single-Layer CP MIMO Antenna	25–29.5	$1.0\lambda_0 \times 1.0\lambda_0 \times 0.04\lambda_0$	23.4	11	—	—	—	—	—	—
[113]	Wideband Antipodal Vivaldi Antenna	15–41.3	50 × 24 × 0.51	9.25–15.26	—	—	—	—	—	—	—

- ***Diversity Performance Assessment:*** Overcoming challenges related to diversity performance assessment is crucial. Ensuring reliable communication in diverse environments requires advancements in MIMO antenna designs to address issues such as non-constant scattering parameters and wide beamwidth.
- ***Dielectric Substrate Selection:*** The review acknowledges the use of Rogers/FR-4 substrates and explores alternatives like geopolymers to achieve broader bandwidth. Selecting suitable dielectric materials is critical for enhancing the overall performance and bandwidth of millimeter-wave antennas.
- ***Flexible Substrate Challenges:*** The emerging trend of flexible substrates, such as Rogers 6006 or textiles, faces challenges like bending losses and radiation changes. Research in this area is needed to address these issues and unlock the potential of flexible MIMO designs at millimeter-wave frequencies.

5. CONCLUSION AND FUTURE SCOPE

This paper provides the comprehensive review of diverse MIMO antennas, encompassing slot/patch/stub antennas, defected ground antennas, MIMO Antenna Array, dielectric resonator antennas (DRA), and Meta-surface/metamaterial-based antennas, with a specific concentration on their application in mmWave scenarios. The overarching objective has been to address an array of challenges intrinsic to this domain, including issues pertaining to diversity performance assessment, non-constant scattering parameters, wide beamwidth, average gain, and other pertinent factors. This extensive examination not only brings attention to the current obstacles but also emphasizes the fundamental standards that must be met in order to advance the development and deployment of MIMO antennas. As a result, it offers developers and practitioners 5G networks valuable insights that are instrumental in achieving optimal performance.

Recognizing the pivotal role of MIMO antennas in the successful deployment of 5G technology, it is imperative that these antennas exhibit effectiveness across a broad frequency spectrum, substantial amplification capabilities, and the ability to emit radiation in a focused manner. Addressing these concerns in the context of future MIMO designs necessitates a strategic emphasis on compactness to fulfill diversity parameters adequately.

REFERENCES

[1] Shah, S. C., "Private mobile edge cloud for 5G network applications," *Internet Technology Letters*, Vol. 2, No. 5, Aug. 2019.

[2] "5G spectrum sold, get ready to roll out for consumers: Centre to telcos, NDTV.com," Sep. 2022. [Online]. Available: https://www.ndtv.com/business/5g-update-5g-spectrum-sold-get-ready-to-roll-out-for-consumerscentre-to-telcos-3264323.

[3] "5G spectrum auction ends, govt earns over Rs 1.5 Lakh Cr; Reliance Jio top bidder, The Indian Express, Aug. 01, 2022," Sep. 2022. [Online]. Available: https://indianexpress.com/article/business/india-concludes-19-bln-5g-spectrum-auction-8064216/.

[4] I.T.U. Statistics, 2023. [Online]. Available: https://www.itu.int:443/en/ITU-D/Statistics/Pages/stat/default.aspx.

[5] "World internet users statistics and 2022 world population stats," Jun. 2022. [Online]. Available: https://www.internetworldstats.com/stats.htm.

[6] Hanson, H. and N. C. Kraus, "Long-term evolution of a long-term evolution model," *Journal of Coastal Research*, No. 59, 118–129, 2011.

[7] Brenner, D., "Global 5G spectrum update," *SVP, Spectrum Strategy & Technology Policy*, 28, 2020.

[8] Forge, S. and K. Vu, "Forming a 5G strategy for developing countries: A note for policy makers," *Telecommunications Policy*, Vol. 44, No. 7, 101975, Aug. 2020.

[9] Pi, Z. and F. Khan, "An introduction to millimeter-wave mobile broadband systems," *IEEE Communications Magazine*, Vol. 49, No. 6, 101–107, Jun. 2011.

[10] Du, J. and R. A. Valenzuela, "How much spectrum is too much in millimeter wave wireless access," *IEEE Journal on Selected*

Areas in Communications, Vol. 35, No. 7, 1444–1458, Jul. 2017.

[11] "Most internet users by country," in *Statistics*, https://www.statista.com/statistics/262966/number-of-internet-users-in-selected-countries/, Oct. 2023.

[12] Shariff, B. G. P., P. R. Mane, P. Kumar, T. Ali, and M. G. N. Alsath, "Planar MIMO antenna for mmWave applications: Evolution, present status & future scope," *Heliyon*, Vol. 9, No. 2, Feb. 2023.

[13] Sudhamani, C., M. Roslee, J. J. Tiang, and A. U. Rehman, "A survey on 5G coverage improvement techniques: Issues and future challenges," *Sensors*, Vol. 23, No. 4, 2356, Feb. 2023.

[14] Rajiv, "Applications of millimeter waves and future," Jul. 2023, https://www.rfpage.com/applications-of-millimeter-waves-future/.

[15] Cetnar, J. S., "Atmospheric effects on the propagation of mmW and sub-mmW radiation," Ph.D. dissertation, Wright State University, 2010.

[16] Oladimeji, T. T., P. Kumar, and N. O. Oyie, "Propagation path loss prediction modelling in enclosed environments for 5G networks: A review," *Heliyon*, Vol. 8, No. 11, 2022.

[17] Kumar, A. and M. Gupta, "A review on activities of fifth generation mobile communication system," *Alexandria Engineering Journal*, Vol. 57, No. 2, 1125–1135, Jun. 2018.

[18] Parkvall, S., E. Dahlman, A. Furuskar, and M. Frenne, "NR: The new 5G radio access technology," *IEEE Communications Standards Magazine*, Vol. 1, No. 4, 24–30, 2017.

[19] Zada, M., I. A. Shah, and H. Yoo, "Integration of sub-6-GHz and mm-Wave bands with a large frequency ratio for future 5G MIMO applications," *IEEE Access*, Vol. 9, 11 241–11 251, 2021.

[20] Dybdal, R., "Millimeter wave antenna technology," *IEEE Journal on Selected Areas in Communications*, Vol. 1, No. 4, 633–644, Sep. 1983.

[21] Sheriff, N., S. K. A. Rahim, H. T. Chattha, and T. K. Geok, "Multiport single element MIMO antenna systems: A review," *Sensors*, Vol. 23, No. 2, 747, Jan. 2023.

[22] Desai, A., T. Upadhyaya, and R. Patel, "Compact wideband transparent antenna for 5G communication systems," *Microwave and Optical Technology Letters*, Vol. 61, No. 3, 781–786, Mar. 2019.

[23] Esmail, B. A. F., S. Koziel, and S. Szczepanski, "Overview of planar antenna loading metamaterials for gain performance enhancement: The two decades of progress," *IEEE Access*, Vol. 10, 27 381–27 403, 2022.

[24] Ni, C., W. W. Wang, Y. C. Zheng, J. Ding, K. Cao, and B. Liu, "A millimeter-wave antipodal linearly tapered slot antenna array for 5G wireless communication," *International Journal of Antennas and Propagation*, Vol. 2023, Article ID 6 227 251, 12 pages, Jul. 2023.

[25] Althuwayb, A. A., "MTM- and SIW-inspired bowtie antenna loaded with AMC for 5G mm-Wave applications," *International Journal of Antennas and Propagation*, Vol. 2021, Article ID 6 658 819, 7 pages, Jan. 2021.

[26] Shariff, B. G. P., T. Ali, P. R. Mane, and P. Kumar, "Array antennas for mmWave applications: A comprehensive review," *IEEE Access*, Vol. 10, 126 728–126 766, 2022.

[27] Levine, E., G. Malamud, S. Shtrikman, and D. Treves, "A study of microstrip array antennas with the feed network," *IEEE Transactions on Antennas and Propagation*, Vol. 37, No. 4, 426–434, Apr. 1989.

[28] Ren, Q., B. Qian, X. Chen, X. Huang, Q. Li, J. Zhang, and A. A. Kishk, "Linear antenna array with large element spacing for wide-angle beam scanning with suppressed grating lobes," *IEEE Antennas and Wireless Propagation Letters*, Vol. 21, No. 6, 1258–1262, Jun. 2022.

[29] Ishteyaq, I. and K. Muzaffar, "Multiple input multiple output (MIMO) and fifth generation (5G): An indispensable technology for sub-6 GHz and millimeter wave future generation mobile terminal applications," *International Journal of Microwave and Wireless Technologies*, Vol. 14, No. 7, 932–948, Sep. 2022.

[30] Andrews, J. G., S. Buzzi, W. Choi, S. V. Hanly, A. Lozano, A. C. K. Soong, and J. C. Zhang, "What will 5G be?" *IEEE Journal on Selected Areas in Communications*, Vol. 32, No. 6, 1065–1082, Jun. 2014.

[31] Rappaport, T. S., *Wireless Communications: Principle and Practice*, Vol. 2, Prentice Hall PTR, 1996.

[32] Islam, M. J., "Performance analysis of diversity techniques for wireless communication system," Blekinge Institute of Technology, 2012.

[33] Yu, X., W. Tan, Y. Wang, X. Liu, Y. Rui, and M. Chen, "Performance analysis of distributed antenna systems with antenna selection over MIMO Rayleigh fading channel," *KSII Transactions on Internet and Information Systems*, Vol. 8, No. 9, 3016–3033, Sep. 2014.

[34] Zeng, E.-L., S.-H. Zhu, X.-W. Liao, and J. Wang, "Grouped multiuser diversity for spatial multiplexing MIMO systems," *Journal of Electronics & Information Technology*, Vol. 30, No. 1, 81–85, Feb. 2011.

[35] Casu, G., L. Tuta, I. Nicolaescu, and C. Moraru, "Some aspects about the advantages of using MIMO systems," in *2014 22nd Telecommunications Forum Telfor (TELFOR)*, 320–323, Belgrade, Serbia, Nov. 2014.

[36] Long, Y., Z. Chen, and J. Fang, "Nonasymptotic analysis of capacity in massive MIMO systems," *IEEE Wireless Communications Letters*, Vol. 4, No. 5, 541–544, Oct. 2015.

[37] Kumar, V., "Nonasymptotic analysis of massive MIMO under different wireless scenarios," Ph.D. dissertation, Doctoral dissertation, 2020.

[38] Lee, W., "Effect of mutual coupling on a mobile-radio maximum ratio diversity combiner with a large number of branches," *IEEE Transactions on Communications*, Vol. 21, No. 3, 266–267, Mar. 1973.

[39] Kumar, A., A. Kumar, and A. Kumar, "Defected ground structure based high gain, wideband and high diversity performance quad-element MIMO antenna array for 5G millimeter-wave communication," *Progress In Electromagnetics Research B*, Vol. 101, 1–16, 2023.

[40] Ghosh, S., G. S. Baghel, and M. V. Swati, "Design of a highly-isolated, high-gain, compact 4-port MIMO antenna loaded with CSRR and DGS for millimeter wave 5G communications," *AEU-International Journal of Electronics and Communications*, Vol. 169, 154721, 2023.

[41] Güler, C. and S. E. Bayer Keskin, "A novel high isolation 4-port compact MIMO antenna with DGS for 5G applications," *Micromachines*, Vol. 14, No. 7, 1309, 2023.

[42] Johansson, M., M. Karreman, and A. Foukaki, "3rd generation partnership project: Coopetition in a developmental standardisation setting," in *Academy of Management Proceedings*, Vol. 2017, No. 1, 11281, Aug. 2017.

[43] Nakano, H. and J. Yamauchi, "Printed slot and wire antennas: A review," *Proceedings of the IEEE*, Vol. 100, No. 7, 2158–2168, Jul. 2012.

[44] Long, Y., Z. Chen, and J. Fang, "Nonasymptotic analysis of capacity in massive MIMO systems," *IEEE Wireless Communications Letters*, Vol. 4, No. 5, 541–544, Oct. 2015.

[45] Deshmukh, A. A., A. Rane, S. Surendran, Y. Bhasin, and V. A. P. Chavali, "Wideband and compact regular shape microstrip antennas employing rectangular slots cut bow-tie shape ground plane," *Progress In Electromagnetics Research B*, Vol. 100, 155–172, 2023.

[46] Kumar, R., G. S. Saini, and D. Singh, "Compact tri-band patch antenna for Ku band applications," *Progress In Electromagnetics Research C*, Vol. 103, 45–58, 2020.

[47] Wa'il, A., R. M. Shaaban, and Z. A. Ahmed, "A modified E-shaped microstrip patch antenna for dual band in X- and Ku-bands applications," in *Journal of Physics: Conference Series*, Vol. 1234, No. 1, 012028, IOP Publishing, Jul. 2019.

[48] Dastranj, A. and H. Abiri, "Bandwidth enhancement of printed E-shaped slot antennas fed by CPW and microstrip line," *IEEE Transactions on Antennas and Propagation*, Vol. 58, No. 4, 1402–1407, Apr. 2010.

[49] Tong, K.-F. and T.-P. Wong, "Circularly polarized U-slot antenna," *IEEE Transactions on Antennas and Propagation*, Vol. 55, No. 8, 2382–2385, Aug. 2007.

[50] Xu, R., J.-Y. Li, J.-J. Yang, K. Wei, and Y.-X. Qi, "A design of U-shaped slot antenna with broadband dual circularly polarized radiation," *IEEE Transactions on Antennas and Propagation*, Vol. 65, No. 6, 3217–3220, Jun. 2017.

[51] Sung, Y. J., "Bandwidth enhancement of a wide slot using fractal-shaped sierpinski," *IEEE Transactions on Antennas and Propagation*, Vol. 59, No. 8, 3076–3079, Aug. 2011.

[52] Chen, W.-L., G.-M. Wang, and C.-X. Zhang, "Bandwidth enhancement of a microstrip-line-fed printed wide-slot antenna with a fractal-shaped slot," *IEEE Transactions on Antennas and Propagation*, Vol. 57, No. 7, 2176–2179, Jul. 2009.

[53] Kobal, E., R.-J. Liu, C. Yu, and A. Zhu, "A high isolation, low-profile, triple-port SIW based annular slot antenna for millimeter-wave 5G MIMO applications," *IEEE Access*, Vol. 10, 89 458–89 464, 2022.

[54] Wang, J., Y. Li, and J. Wang, "A low-profile dual-mode slot-patch antenna for 5G millimeter-wave applications," *IEEE Antennas and Wireless Propagation Letters*, Vol. 21, No. 3, 625–629, Mar. 2022.

[55] Jabeen, S. and Q. U. Khan, "An integrated MIMO antenna design for sub-6 GHz & millimeter-wave applications with high isolation," *AEU-International Journal of Electronics and Communications*, Vol. 153, 154247, Aug. 2022.

[56] Jakhar, J., T. Jhajharia, and B. Gupta, "Asymmetric flare shape patch MIMO antenna for millimeter wave 5G communication systems," *Progress In Electromagnetics Research C*, Vol. 136, 75–86, 2023.

[57] Sehrai, D. A., M. Abdullah, A. Altaf, S. H. Kiani, F. Muhammad, M. Tufail, M. Irfan, A. Glowacz, and S. Rahman, "A novel high gain wideband MIMO antenna for 5G millimeter wave applications," *Electronics*, Vol. 9, No. 6, 1031, 2020.

[58] Patel, A., A. Vala, A. Desai, I. Elfergani, H. Mewada, K. Mahant, C. Zebiri, D. Chauhan, and J. Rodriguez, "Inverted-L shaped wideband MIMO antenna for millimeter-wave 5G applications," *Electronics*, Vol. 11, No. 9, 1387, May 2022.

[59] Jetti, C. R., T. Addepalli, S. R. Devireddy, G. K. Tanimki, A. J. A. Al-Gburi, Z. Zakaria, and P. Sunitha, "Design and analysis of modified U-shaped four element MIMO antenna for dual-band 5G millimeter wave applications," *Micromachines*, Vol. 14, No. 8, 1545, Aug. 2023.

[60] El-Nady, S. M. and A. M. Attiya, "Periodically-stub-loaded microstrip line wideband circularly polarized millimeter wave MIMO antenna," *IEEE Access*, Vol. 10, 20 465–20 472, 2022.

[61] Ali, W., S. Das, H. Medkour, and S. Lakrit, "Planar dual-band 27/39 GHz millimeter-wave MIMO antenna for 5G applications," *Microsystem Technologies*, Vol. 27, No. 1, 283–292, Jan. 2021.

[62] Farooq, U. and A. Lokam, "A compact 26/39 GHz millimeter wave MIMO antenna design for 5G IoT applications," *Journal of Infrared Millimeter and Terahertz Waves*, Vol. 44, No. 5-6, 333–345, Jun. 2023.

[63] Khalid, M., S. I. Naqvi, N. Hussain, M. Rahman, Fawad, S. S. Mirjavadi, M. J. Khan, and Y. Amin, "4-port MIMO antenna with defected ground structure for 5G millimeter wave applications," *Electronics*, Vol. 9, No. 1, 71, Jan. 2020.

[64] Abdullah, A., H. Ahmad, M. Rahman, M. Haris, and M. Salman, "Wideband four-port compact millimeter-wave MIMO antenna configuration through defected ground structure for forthcoming 5G handheld devices," *Progress In Electromagnetics Research C*, Vol. 117, 173–184, 2021.

[65] Patel, A., A. Desai, I. Elfergani, A. Vala, H. Mewada, K. Mahant, S. Patel, C. Zebiri, J. Rodriguez, and E. Ali, "UWB CPW fed 4-port connected ground MIMO antenna for sub-millimeter-wave 5G applications," *Alexandria Engineering Journal*, Vol. 61, No. 9, 6645–6658, Sep. 2022.

[66] Dwivedi, A. K., N. K. Narayaswamy, V. Singh, and M. S. Darmanar, "UWB-MIMO DGS loaded patch antenna with low profile for millimeter-wave applications," *Journal of Electrical Engineering*, Vol. 73, No. 1, 28–35, Feb. 2022.

[67] Sharma, S. and M. Arora, "A millimeter wave elliptical slot circular patch MIMO antenna for future 5G mobile communication networks," *Progress In Electromagnetics Research M*, Vol. 110, 235–247, 2022.

[68] Joseph, J., G. S. Let, C. B. Pratap, and J. J. Winston, "A miniaturized uniplanar MIMO antenna for n79/n46/millimeter-wave applications," *International Journal of Communication Systems*, Vol. 36, No. 9, e5477, Jun. 2023.

[69] Abbas, M. A., A. Allam, A. Gaafar, H. M. Elhennawy, and M. F. A. Sree, "Compact UWB MIMO antenna for 5G millimeter-wave applications," *Sensors*, Vol. 23, No. 5, 2702, Mar. 2023.

[70] Kumar, A., A. Kumar, and A. Kumar, "Defected ground structure based high gain, wideband and high diversity performance quad-element MIMO antenna array for 5G millimeter-wave communication," *Progress In Electromagnetics Research B*, Vol. 101, 1–16, 2023.

[71] Hussain, R., M. Abou-Khousa, N. Iqbal, A. Algarni, S. I. I. Alhuwaimel, A. Zerguine, and M. S. S. Sharawi, "A multiband shared aperture MIMO antenna for millimeter-wave and sub-6 GHz 5G applications," *Sensors*, Vol. 22, No. 5, 1808, Mar. 2022.

[72] Tahat, A., B. Ersan, L. Muhesen, Z. Shakhshir, and T. A. Edwan, "A compact 38 GHz millimetre-wave MIMO antenna array for 5G mobile systems," *Journal of Telecommunications and the Digital Economy*, Vol. 8, No. 3, 44–59, 2020.

[73] Yang, B., Z. Yu, Y. Dong, J. Zhou, and W. Hong, "Compact tapered slot antenna array for 5G millimeter-wave massive MIMO systems," *IEEE Transactions on Antennas and Propagation*, Vol. 65, No. 12, 6721–6727, Dec. 2017.

[74] Kamal, M. M., S. Yang, X.-C. Ren, A. Altaf, S. H. Kiani, M. R. Anjum, A. Iqbal, M. Asif, and S. I. Saeed, "Infinity shell shaped MIMO antenna array for mm-Wave 5G applications," *Electronics*, Vol. 10, No. 2, 165, Jan. 2021.

[75] Bilal, M., S. I. Naqvi, N. Hussain, Y. Amin, and N. Kim, "High-isolation MIMO antenna for 5G millimeter-wave communication systems," *Electronics*, Vol. 11, No. 6, 962, Mar. 2022.

[76] Malviya, L. and P. Gupta, "Millimeter wave high-gain antenna array for wireless applications," *IETE Journal of Research*, Vol. 69, No. 5, 2645–2654, Jul. 2023.

[77] Khan, J., S. Ullah, U. Ali, F. A. Tahir, I. Peter, and L. Matekovits, "Design of a millimeter-wave MIMO antenna array for 5G communication terminals," *Sensors*, Vol. 22, No. 7, 2768, Apr. 2022.

[78] Ud Din, I., M. Alibakhshikenari, B. S. S. Virdee, R. K. R. Jayanthi, S. Ullah, S. Khan, C. H. See, L. Golunski, and S. Koziel, "Frequency-selective surface-based MIMO antenna array for 5G millimeter-wave applications," *Sensors*, Vol. 23, No. 15, 7009, Aug. 2023.

[79] Mandloi, M. S., P. Gupta, A. Parmar, P. Malviya, and L. Malviya, "Beamforming MIMO array antenna for 5G-millimeter-wave application," *Wireless Personal Communications*, Vol. 129, No. 1, 153–172, Mar. 2023.

[80] Keyrouz, S. and D. Caratelli, "Dielectric resonator antennas: Basic concepts, design guidelines, and recent developments at millimeter-wave frequencies," *International Journal of Antennas and Propagation*, Vol. 2016, 2016.

[81] Erfani, E., T. Denidni, S. Tatu, and M. Niroo-Jazi, "A broadband and high gain millimeter-wave hybrid dielectric resonator antenna," in *2016 17th International Symposium on Antenna Technology and Applied Electromagnetics (ANTEM16)*, 1–2, IEEE, Montreal, Canada, Jul. 2016.

[82] Lai, Q., C. Fumeaux, W. Hong, and R. Vahldieck, "60 GHz aperture-coupled dielectric resonator antennas fed by a half-mode substrate integrated waveguide," *IEEE Transactions on Antennas and Propagation*, Vol. 58, No. 6, 1856–1864, 2010.

[83] Bijumon, P. V., Y. M. A. Antar, A. P. Freundorfer, and M. Sayer, "Integrated dielectric resonator antennas for system on-chip applications," in *2007 International Conference on Microelectronics (ICM'07)*, 275–278, IEEE, Cairo, Egypt, Dec. 2007.

[84] Bijumon, P. V., Y. M. M. Antar, A. P. Freundorfer, and M. Sayer, "Dielectric resonator antenna on silicon substrate for system on-chip applications," *IEEE Transactions on Antennas and Propagation*, Vol. 56, No. 11, 3404–3410, Nov. 2008.

[85] Abdulmajid, A. A., S. Khamas, and S. Zhang, "Wideband high-gain millimetre-wave three-layer hemispherical dielectric resonator antenna," *Progress In Electromagnetics Research C*, Vol. 103, 225–236, 2020.

[86] Zubir, I. A., M. Othman, U. Ullah, S. Kamal, M. F. A. Rahman, R. Hussin, M. F. B. M. Omar, A. S. B. Mohammed, M. F. B. Ain, Z. A. Ahmad, and M. Z. Abdullah, "A low-profile hybrid multi-permittivity dielectric resonator antenna with perforated structure for Ku and K band applications," *IEEE Access*, Vol. 8, 151 219–151 228, 2020.

[87] Baldazzi, E., A. Al-Rawi, R. Cicchetti, A. B. Smolders, O. Testa, C. D. J. Van Coevorden Moreno, and D. Caratelli, "A high-gain dielectric resonator antenna with plastic-based conical horn for millimeter-wave applications," *IEEE Antennas and Wireless Propagation Letters*, Vol. 19, No. 6, 949–953, Jun. 2020.

[88] Gong, K. and X. H. Hu, "Low-profile substrate integrated dielectric resonator antenna implemented with PCB process," *IEEE Antennas and Wireless Propagation Letters*, Vol. 13, 1023–1026, 2014.

[89] Keyrouz, S. and D. Caratelli, "Dielectric resonator antennas: Basic concepts, design guidelines, and recent developments at millimeter-wave frequencies," *International Journal of Antennas and Propagation*, Vol. 2016, 6075680, 2016.

[90] Meher, P. R., B. R. Behera, and S. K. Mishra, "Design and its state-of-the-art of different shaped dielectric resonator antennas at millimeter-wave frequency band," *International Journal of RF and Microwave Computer-Aided Engineering*, Vol. 30, No. 7, 22221, Jul. 2020.

[91] Wahab, W. M. A., D. Busuioc, and S. Safavi-Naeini, "Low cost planar waveguide technology-based dielectric resonator antenna (DRA) for millimeter-wave applications: Analysis, design, and fabrication," *IEEE Transactions on Antennas and Propagation*, Vol. 58, No. 8, 2499–2507, Aug. 2010.

[92] Abdel-Wahab, W. M., Y. Wang, and S. Safavi-Naeini, "SIW hybrid feeding network-integrated 2-D DRA array: Simulations and experiments," *IEEE Antennas and Wireless Propagation Letters*, Vol. 15, 548–551, 2016.

[93] Abdel-Wahab, W. M., M. Abdallah, J. Anderson, Y. Wang, H. Al-Saedi, and S. Safavi-Naeini, "SIW-integrated parasitic DRA array: Analysis, design, and measurement," *IEEE Antennas and Wireless Propagation Letters*, Vol. 18, No. 1, 69–73, 2018.

[94] Mazhar, W., D. M. Klymyshyn, G. Wells, A. A. Qureshi, M. Jacobs, and S. Achenbach, "Low-profile artificial grid dielectric resonator antenna arrays for mm-Wave applications," *IEEE Transactions on Antennas and Propagation*, Vol. 67, No. 7, 4406–4417, Jul. 2019.

[95] Abdel-Wahab, W. M., D. Busuioc, and S. Safavi-Naeini, "Millimeter-wave high radiation efficiency planar waveguide series-fed dielectric resonator antenna (DRA) array: Analysis, design, and measurements," *IEEE Transactions on Antennas and Propagation*, Vol. 59, No. 8, 2834–2843, Aug. 2011.

[96] Liu, Y.-T., B. Ma, S. Huang, S. Wang, Z. J. Hou, and W. Wu, "Wideband low-profile connected rectangular ring dielectric resonator antenna array for millimeter-wave applications," *IEEE Transactions on Antennas and Propagation*, Vol. 71, No. 1, 999–1004, 2022.

[97] Dadgarpour, A., B. Zarghooni, B. S. Virdee, T. A. Denidni, and A. A. Kishk, "Mutual coupling reduction in dielectric resonator antennas using metasurface shield for 60-GHz MIMO systems," *IEEE Antennas and Wireless Propagation Letters*, Vol. 16, 477–480, 2016.

[98] Farahani, M., J. Pourahmadazar, M. Akbari, M. Nedil, A. R. Sebak, and T. A. Denidni, "Mutual coupling reduction in millimeter-wave MIMO antenna array using a metamaterial polarization-rotator wall," *IEEE Antennas and Wireless Propagation Letters*, Vol. 16, 2324–2327, 2017.

[99] Pan, Y. M., X. Qin, Y. X. Sun, and S. Y. Zheng, "A simple decoupling method for 5G millimeter-wave MIMO dielectric resonator antennas," *IEEE Transactions on Antennas and Propagation*, Vol. 67, No. 4, 2224–2234, Apr. 2019.

[100] Zhang, Y., J.-Y. Deng, M.-J. Li, D. Sun, and L.-X. Guo, "A MIMO dielectric resonator antenna with improved isolation for 5G mm-Wave applications," *IEEE Antennas and Wireless Propagation Letters*, Vol. 18, No. 4, 747–751, Apr. 2019.

[101] Murthy, N., "Improved isolation metamaterial inspired mm-Wave MIMO dielectric resonator antenna for 5G application," *Progress In Electromagnetics Research C*, Vol. 100, 247–261, 2020.

[102] Chu, H. and Y.-X. Guo, "A novel approach for millimeter-wave dielectric resonator antenna array designs by using the substrate integrated technology," *IEEE Transactions on Antennas and Propagation*, Vol. 65, No. 2, 909–914, 2016.

[103] Gaya, A., M. H. Jamaluddin, B. Alali, and A. A. Althuwayb, "A novel wide dual band circularly polarized dielectric resonator antenna for millimeter wave 5G applications," *Alexandria En-*

gineering Journal, Vol. 61, No. 12, 10 791–10 803, Dec. 2022.

[104] Huang, R. Z., J. W. Zhang, and C. Zhang, "Dual-band circularly polarized hybrid dielectric resonator antenna for 5G millimeter-wave applications," *Electronics*, Vol. 11, No. 11, 1761, 2022.

[105] Zhao, G., Y. Zhou, J. R. Wang, and M. S. Tong, "A circularly polarized dielectric resonator antenna based on quasi-self-complementary metasurface," *IEEE Transactions on Antennas and Propagation*, Vol. 70, No. 8, 7147–7151, Aug. 2022.

[106] Xu, H., Z. Chen, H. Liu, L. Chang, T. Huang, S. Ye, L. Zhang, and C. Du, "Single-fed dual-circularly polarized stacked dielectric resonator antenna for K/Ka-band UAV satellite communications," *IEEE Transactions on Vehicular Technology*, Vol. 71, No. 4, 4449–4453, Apr. 2022.

[107] Alanazi, M. D., "A review of dielectric resonator antenna at mm-Wave band," *ENG*, Vol. 4, No. 1, 843–856, 2023.

[108] Kumar, S. and H. Singh, "A comprehensive review of metamaterials/metasurface-based MIMO antenna array for 5G millimeter-wave applications," *Journal of Superconductivity and Novel Magnetism*, Vol. 35, No. 11, 3025–3049, Nov. 2022.

[109] Singh, M., S. Singh, and M. T. Islam, "CSRR loaded high gained 28/38 GHz printed MIMO patch antenna array for 5G millimeter wave wireless devices," *Microelectronic Engineering*, Vol. 262, 111829, Jun. 2022.

[110] Tadesse, A. D., O. P. Acharya, and S. Sahu, "A compact planar four-port MIMO antenna for 28/38 GHz millimeter-wave 5G applications," *Advanced Electromagnetics*, Vol. 11, No. 3, 16–25, Aug. 2022.

[111] Sharawi, M. S., "Current misuses and future prospects for printed multiple-input, multiple-output antenna systems," *IEEE Antennas and Propagation Magazine*, Vol. 59, No. 2, 162–170, Apr. 2017.

[112] Esmail, B. A. and S. Koziel, "High isolation metamaterial-based dual-band MIMO antenna for 5G millimeter-wave applications," *AEU-International Journal of Electronics and Communications*, Vol. 158, 154470, Jan. 2023.

[113] Tariq, S., S. I. Naqvi, N. Hussain, and Y. Amin, "A metasurface-based MIMO antenna for 5G millimeter-wave applications," *IEEE Access*, Vol. 9, 51 805–51 817, 2021.

[114] Hussain, N., M.-J. Jeong, A. Abbas, and N. Kim, "Metasurface-based single-layer wideband circularly polarized MIMO antenna for 5G millimeter-wave systems," *IEEE Access*, Vol. 8, 130 293–130 304, 2020.

[115] Kumar, S. and A. S. Dixit, "Wideband antipodal Vivaldi antenna using metamaterial for micrometer and millimeter wave applications," *Journal of Infrared Millimeter and Terahertz Waves*, Vol. 42, No. 9-10, 974–985, Sep. 2021.

[116] Juneja, S., R. Pratap, and R. Sharma, "Design of a highly directive, wideband and compact endfire antenna array for 5G applications," in *2022 IEEE International Conference of Electron Devices Society Kolkata Chapter (EDKCON)*, 558–562, IEEE, Nov. 2022.

[117] Juneja, S. and R. Sharma, "Study of techniques to improve performance of patch antennas for 5G applications at millimeter wave (mmW) frequencies," in *IOP Conference Series: Materials Science and Engineering*, Vol. 1022, No. 1, 012033, IOP Publishing, 2021.